5400 J. Med. Chem. 2010, 53, 5400–5421
DOI: 10.1021/jm100075z

Journal of Medicinal Chemistry Article

Identification of Orally Available Naphthyridine Protein Kinase D Inhibitors

Erik L. Meredith,[†] Ophelia Ardayfio,[†] Kimberly Beattie,[†] Markus R. Dobler,[†] Istvan Enyedy,[†] Christoph Gaul,[‡] Vinayak Hosagrahara,[†] Charles Jewell,[†] Keith Koch,[§] Wendy Lee,[†] HansJoerg Lehmann,[‡] Timothy A. McKinsey,[§] Karl Miranda,[†] Nikos Pagratis,[§] Margaret Pancost,[†] Anup Patnaik,[†] Dillon Phan,[§] Craig Plato,[§] Ming Qian,[†] Vasumathy Rajaraman,[†] Chang Rao,[†] Olga Rozhitskaya,[†] Thomas Ruppen,[‡] Jie Shi,[†] Sarah J. Siska,[†] Clayton Springer,[†] Maurice van Eis,[‡] Richard B. Vega,[†] Anette von Matt,[‡] Lihua Yang,[†] Taeyoung Yoon,[†] Ji-Hu Zhang,[†] Na Zhu,[†] and Lauren G. Monovich*,[†]

[†]*Novartis Institutes for BioMedical Research, 100 Technology Square, Cambridge, Massachusetts 02139,* [‡]*Novartis Institutes for BioMedical Research, Basel, Switzerland, and* [§]*Gilead Colorado, Inc., 3333 Walnut Street, Boulder, Colorado 80301*

Received January 18, 2010

A novel 2,6-naphthyridine was identified by high throughput screen (HTS) as a dual protein kinase C/D (PKC/PKD) inhibitor. PKD inhibition in the heart was proposed as a potential antihypertrophic mechanism with application as a heart failure therapy. As PKC was previously identified as the immediate upstream activator of PKD, PKD vs PKC selectivity was essential to understand the effect of PKD inhibition in models of cardiac hypertrophy and heart failure. The present study describes the modification of the HTS hit to a series of prototype pan-PKD inhibitors with routine 1000-fold PKD vs PKC selectivity. Example compounds inhibited PKD activity in vitro, in cells, and in vivo following oral administration. Their effects on heart morphology and function are discussed herein.

Introduction

Heart failure,[1] a leading cause of death in industrialized nations, is characterized by increased cardiac size and loss of cardiovascular function. In patients with cardiac dysfunction, it is unknown whether increased cardiac size or cardiac hypertrophy is causative or compensatory for cardiac dysfunction,[2] but the enlarged heart, specifically hypertrophy of the left ventricle, is an independent risk factor for adverse cardiac events.[3] Further, reduction of existing cardiac hypertrophy decreases mortality.[4] Cardiac hypertrophy does not reflect hyperplasia of the cardiac muscle cells, or cardiac myocytes, but rather hypertrophy of the individual myocytes.[5] Thus, aberrant hypertrophic signaling pathways in the cardiac myocyte present attractive targets to intercept pathological cardiac hypertrophy and to explore the effect on cardiac function.[6]

Within the normal adult cardiac myocyte, the transcription factor myocyte enhancer factor 2 (MEF2[a]) dependent gene expression is repressed by association with class IIa histone deacetylases (HDACs 4, 5, 7, and 9).[7] In failing hearts, derepression of MEF2 is believed to be a key player in adverse cardiac remodeling, including hypertrophy. In accordance with this hypothesis, MEF2D$^{-/-}$ mice are resistant to cardiac hypertrophy induced by stresses such as chronic β-adrenergic stimulation and pressure overload.[8] Conversely, targeted disruption of the MEF2 repressor HDACs, including HDAC5, sensitizes mice to pathological cardiac growth.[9] Cellular localization of class IIa HDACs is controlled by phosphorylation state; phosphorylation of its nuclear localization sequence (NLS) targets HDAC5 for nuclear export to the cytosol, thereby relieving repression of the transcription factor MEF2.[10] In support of this hypothesis, cardiac myocytes expressing phosphorylation-resistant (e.g., Ser → Ala mutant) HDAC5 resist stress-induced hypertrophy.

The subsequent search for the HDAC5 kinase identified the serine/threonine kinase, protein kinase D1 (PKD1),[11] one of three PKD isoforms (including PKDs 2 and 3) from the calmodulin kinase family. The role of PKD1 in pathologic signaling is supported by both gain and loss of function studies in isolated cardiac myoctes and in vivo. For example, in isolated cardiac myocytes, knockdown of PKD1 prevents agonist-induced hypertrophy. In vivo, loss of PKD1 protects mice from pressure overload-induced hypertrophy resulting from surgical banding of the thoracic aorta (TAB). Conversely, transgenic mice overexpressing constitutively active PKD1 develop cardiac dysfunction. By preventing phosphorylation and nuclear export of the MEF2 repressor HDAC5, PKD1 inhibitors are anticipated to control activity of the transcription factor MEF2 and the consequent pathological cardiac hypertrophy and dysfunction.

At the inception of the present study, pan PKC inhibitors, such as Gö-6976 **1**[12] (Figure 1), had been described as a dual PKC/PKD inhibitors. Subsequently, additional PKD inhibitors[13] and an allosteric series exemplified by CID755673[14] have been disclosed. PKC isoforms are described as immediate upstream activator kinases of PKD,[15−17] so PKD vs PKC selectivity, unknown at the inception of the present study, served as an important determinant for a proof of concept PKD inhibitor. Encouragingly, the PKC family, which

*To whom correspondence should be addressed. Phone: 617-871-7606. Fax: 617-871-7045. E-mail: lauren.monovich@novartis.com.

[a] Abbreviations: PKD, protein kinase D; PKC, protein kinase C; TAB, thoracic aortic banded; DSS, Dahl salt-sensitive; HDAC, histone deacetylase; MEF2, myocyte enhancer factor 2; GFP, green fluorescence proteint; LV, left ventricle; TL, tibia length; IVRT, isovolumic relaxation time; MAP, mean arterial pressure; PMA, phorbol 12-myristate 13-acetate; PE, phenylephrine; PGF2α, prostaglandin F2α; ET-1, endothelin-1; LPA, lipopolysaccharide A; PMBCs, peripheral blood mononuclear cells; HTS, high throughput screen.

 Published on Web 07/14/2010 © 2010 American Chemical Society

belongs to the AGC group of kinases, is not closely related to the PKDs, which belong to the calmodulin (CaMK) group of kinases.[18] Conversely, an ATP-competetive inhibitor must distinguish between close sequence homology near the hing-binding regions of the PKCs and PKDs, as in the sequences VMEFLNG and VMEKLHG for PKCδ and PKD1, respectively. The methionine (M) gatekeeper residue is the most common among both the AGC and CaMK kinase groups.[19] Similar to the dual PKC and PKDs inhibitors described in the literature, an HTS from the Novartis archive identified novel 2,6-naphthyridine **2** as a dual inhibitor of PKC and PKD (Figure 1), with 10-fold higher potency vs novel PKC isoforms, such as PKCδ, than PKD (Table 1). Herein, we describe the optimization of **2** to prototype PKD inhibitors with oral availability and 1000-fold selectivity vs PKC isoforms.

Chemistry

The synthesis of **2** and analogues began with pyridine oxide **3**, which underwent methylation followed by attack of cyanide to afford compound **4** (Scheme 1). Nitrile **4** was efficiently converted to the *tert*-butylamide **5** by treatment with *t*-BuOH in concentrated H_2SO_4. Alternatively, compound **5** was accessed from isonicotinic acid **6** by formation of the *tert*-butylamide followed by amide-directed lithiation and trapping with MeI. Deprotonation of compound **5** with *n*-BuLi and treatment with ester **7a** or ester **7b** afforded ketone **8a** or ketone **8b**, respectively. Ring closure with loss of *tert*-butylamine and dehydration to the pyranone occurred with heating in DMF, followed by heating in AcOH. Treatment of the pyrido-pyranones with 25% NH_3 in EtOH afforded the 2,6-naphthyridones, which were successfully halogenated by treatment with $POBr_3$ to give 1-bromo-2,6-naphthyridine **9a** or with $POCl_3$ to give the 1-chloro-2,6-naphthyridines **9b** and **9c**.

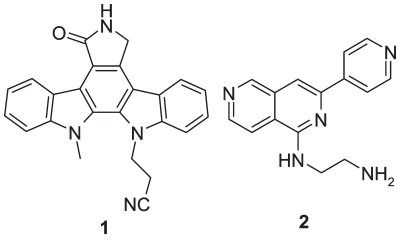

Figure 1. PKD inhibitor structures.

Displacement of the halogen of **9a** or **9b** with nitrogen nucleophiles, such as BOC-protected ethylenediamine, aminopropanol, or BOC-piperazine, afforded 1-amino-2,6-naphthyridines **10a**–**c**. Acidic deprotection of the BOC amines **10a** and **10c** afforded PKD inhibitors **2** and **11**, respectively. Likewise, chloride **9c** was treated with nitrogen nucleophiles to afford **12a**–**c**. Buchwald amination of 2-chloropyridines **12a**–**c** with methylamine, cyclohexylamine, or 4-aminotetrahydropyran gave inhibitors **13**. Compounds **13** were further elaborated as indicated, for example, by acidic deprotection of **13b** or **13e** to give **13c** and **13f**, respectively. Borch reduction of secondary amines **13c** and **13f** gave tertiary amines **13d** and **13g**, respectively.

A similar reaction sequence was used to vary the placement of nitrogen within the core naphthyridine (Scheme 2). *N*-*tert*-Butyl-2-methylbenzamide **14a** or aza analogues **14b**–**d** (where A, B, or E equals nitrogen) were lithiated and trapped with 2-chloroisonicotinic acid methyl ester **7b** as above. The crude ketones **15a**–**d** were directly treated with hot AcOH to effect cyclocondensation to yield pyrido-pyranones, which were then converted to naphthyridones **16a**–**d** by treatment with ammonia in MeOH. To synthesize the quinazoline-containing analogue, treatment of nitrile **17** with HCl in methanol gave imidate **18**, which was condensed with anthranilic acid **19** to afford the quinazolinone **20**. Compounds **16a**–**d** and **20** were chlorinated with $POCl_3$ and treated with BOC-piperazine

Table 1. PKD, PKC, and HDAC Nuclear Export Activity

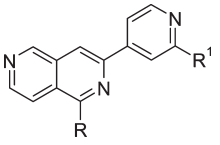

			IC_{50} (nM)			
Cpd	R	R^1	PKD1	PKCα	PKCδ	HDAC exp
1	-	-	27	3.7	446	62
2	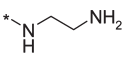	H	321	900	20	5420
10b	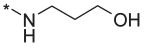	H	>40000	1000	963	>10000
13a	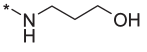		764	1000	1000	>10000
11		H	59	1000	31	2096
12c		Cl	50	1000	1000	1000
13c		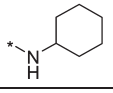	0.6	1000	881	32

The crude ketones **15a**–**d** were directly treated with hot AcOH to effect cyclocondensation to yield pyrido-pyranones, which were then converted to naphthyridones **16a**–**d** by treatment with ammonia in MeOH. To synthesize the quinazoline-containing analogue, treatment of nitrile **17** with HCl in methanol gave imidate **18**, which was condensed with anthranilic acid **19** to afford the quinazolinone **20**. Compounds **16a**–**d** and **20** were chlorinated with $POCl_3$ and treated with BOC-piperazine

Scheme 1. Synthesis of the 2,6-Naphthyridines[a]

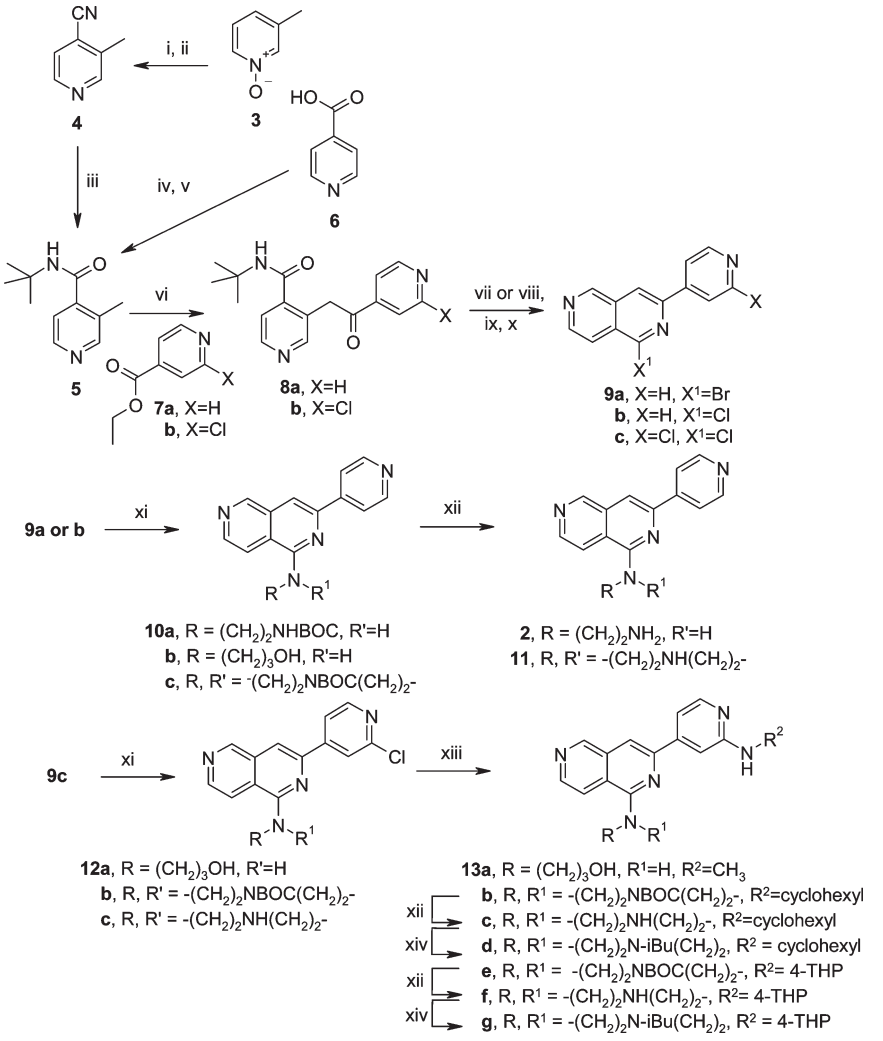

[a] Reagents and conditions: (i) $(MeO)_2SO_2$, EtOH, H_2O, 60 °C, 18 h; (ii) KCN, EtOH, H_2O, 18 h; (iii) *t*-BuOH, conc H_2SO_4, 70 °C, 3 h; (iv) ethyl chloroformate, Et_3N, CH_2Cl_2, then *t*-$BuNH_2$; (v) *n*-BuLi, then MeI; (vi) *n*-BuLi, THF, −70 °C; (vii) DMF, reflux; (viii) AcOH, 100 °C; (ix) 25% NH_3, EtOH; (x) $POBr_3$ or $POCl_3$, Me_4NCl, 110 °C; (xi) $HNRR^1$, Et_3N, EtOH, reflux; (xii) TFA, CH_2Cl_2; (xiii) H_2NR^2, $Pd(OAc)_2$, *t*-BuOK, BINAP, $PhCH_3$, 85 °C; (xiv) isobutyraldehyde, $NaBH(OAc)_3$, $Cl(CH_2)_2Cl$.

to afford **21a**−**e**. As above, elaboration of chloropyridines **21a**−**e** was accomplished by Buchwald amination with cyclohexlyamine. Removal of the BOC-protecting group gave inhibitors **22a**−**e**.

Exploration of additional diversity at the 1-position of the naphthyridine was enabled as described in Schemes 3 and 4. Selective displacement of the 1-chloronaphthyridine **9c** with methoxide afforded **23**, which was reacted with cyclohexylamine utilizing palladium catalysis, demethylated with wet *t*-BuOK, and chlorinated with $POCl_3$ to afford **24** (Scheme 3). Nucleophilic substitution of chloride **24** with a series of cyclic amines afforded inhibitors **13h**−**j**. By analogy to Scheme 1, direct treatment of dichloride **9c** with amines gave intermediates **12d**−**i**, which were converted to targets **13k**−**q** by methods described above. In addition, peptide coupling of piperazine **13f** to BOC-glycine and subsequent BOC removal afforded target **13r**.

Reaction of **9c** with piperidine-4-carboxylic acid derivatives yielded intermediates **12j**−**l** (Scheme 4). Amides **12j** and **12k** were subjected to Pd-catalyzed coupling to cyclohexylamine or 4-aminotetrahydropyran to give compounds **13s-u** (Scheme 4). Alternatively, ester **12l** was converted to a series of target amides **13v**−**ae**. The ester was either saponifed and coupled to the amine using PyBOP or converted directly by treatment of the amine in the presence of Me_3Al. Compounds **13ac** and **13ae** were generated by acidic deprotection of **13ab** and **13ad**, respectively.

Compound Evaluation

In vitro, compounds were evaluated for their ability to inhibit the target PKD1, PKD isoforms 2 and 3, and representative PKC isoforms PKCα and PKCδ. All compounds in the present study were found to competitively inhibit the entire PKD family[18] (isoforms 1, 2, and 3) with similar potency, consistent with the high sequence identity among PKDs 1, 2, and 3. The sequences of the PKD2 and PKD3 kinase domains are 91% and 94% identical, respectively, to that of PKD1.[20] Only the PKD1 activity is reported for clarity, but reference throughout the text to PKD inhibition will represent pan-PKD inhibition. The HDAC nuclear export assay, a cellular readout of PKD activity, monitored the ability of the inhibitors to prevent PGF2α-stimulated nuclear export of GFP-HDAC5 in the cardiac myocyte.

In vivo, selected compounds were evaluated for their ability to block cardiac hypertrophy with daily administration for

Scheme 2. Synthesis of Alternative Cores[a]

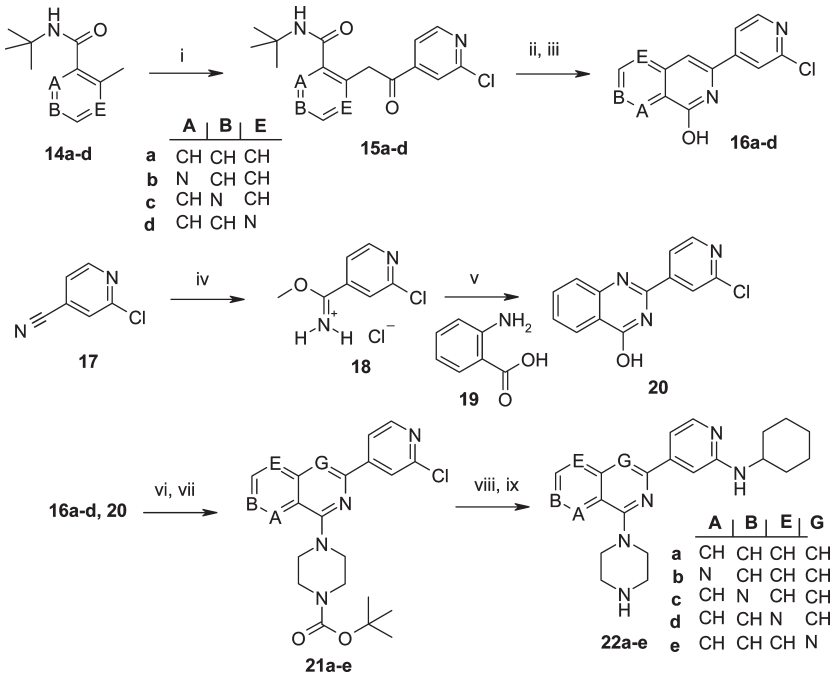

[a] Reagents and conditions: (i) *n*-BuLi, **7b**, THF, −70 °C; (ii) AcOH, 100 °C; (iii) 25% NH_3, EtOH; (iv) HCl, MeOH, dioxane; (v) Na, MeOH; (vi) $POCl_3$, Me_4NCl, 110 °C; (vii) BOC piperazine, Et_3N, EtOH, reflux; (viii) cyclohexylamine, $Pd(OAc)_2$, *t*-BuOK, BINAP, $PhCH_3$, 85 °C; (ix) TFA, CH_2Cl_2.

Scheme 3. Installation of Groups on the 1-Naphthyridine[a]

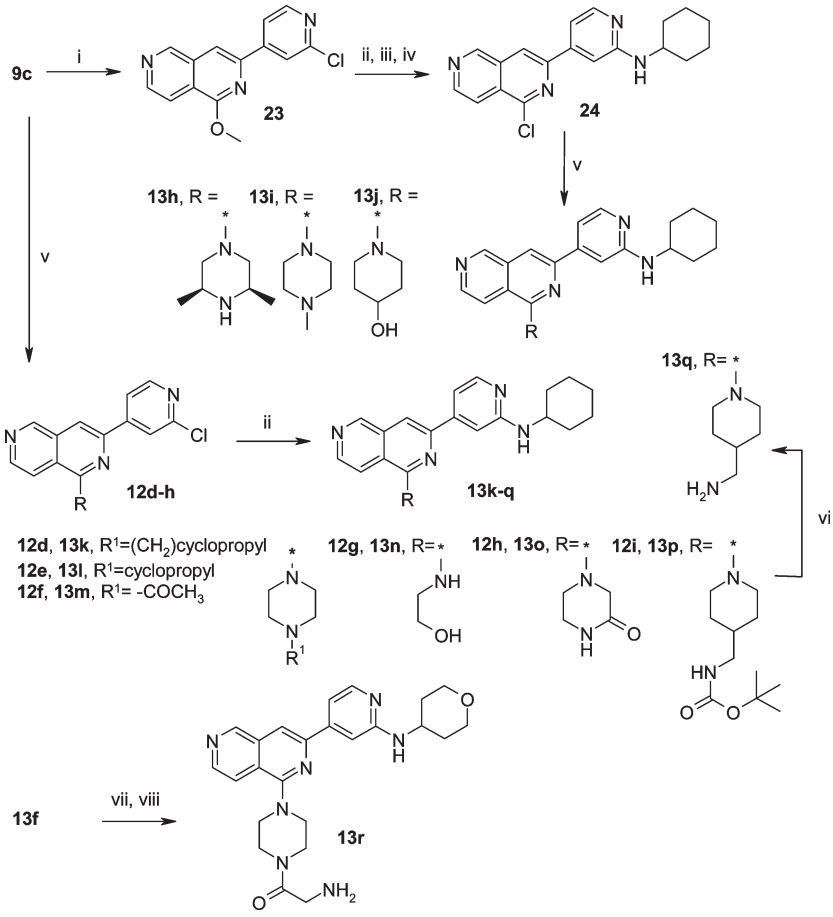

[a] Reagents and conditions: (i) NaOMe, MeOH; (ii) cyclohexylamine, $Pd(OAc)_2$, *t*-BuOK, BINAP, $PhCH_3$, 85 °C; (iii) *t*-BuOK, *t*-BuOH, THF; (iv) $POCl_3$, Me_4NCl, 110 °C; (v) amine, Et_3N, EtOH, reflux; (vi) TFA, CH_2Cl_2; (vii) *N*-BOC-glycine, HBTU, Et_3N; (viii) formic acid.

Scheme 4. Synthesis of 1-Naphthyridines with Pendent Amides and Amide Isosteres[a]

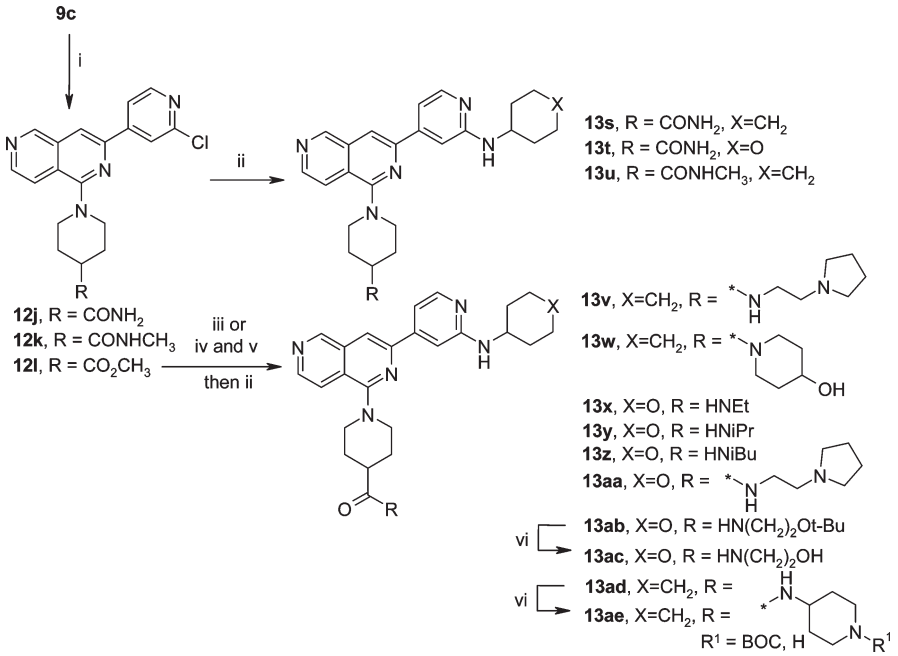

[a] Reagents and conditions: (i) amine, Et_3N, EtOH, reflux; (ii) amine, $Pd(OAc)_2$, *t*-BuOK, BINAP, $PhCH_3$, 85 °C; (iii) amine, Me_3Al; (iv) LiOH, THF, water; (v) amine, PyBop, HOBt; (vi) TFA, CH_2Cl_2; (vii) MsCl.

14 days in a rat model of disease. The two rat models utilized in the present study were the TAB rat, a surgical model of pressure-overload-induced cardiac hypertrophy, recalling that PKD1 knockout was shown to blunt cardiac hypertrophy in the TAB mouse. A second model, the Dahl salt-sensitive (DSS) rat, is a genetic model of high salt-induced hypertension and cardiac hypertrophy. In all rat studies, the effect of compound treatment on blood pressure was monitored to control for the anticipated benefit of antihypertensives on cardiac hypertrophy in both models.

Results

The reported reference PKC/PKD dual inhibitor **1** showed activity vs PKD (IC_{50} = 27 nM) and PKC isoforms (Table 1), as well as the cellular readout of HDAC nuclear export (IC_{50} = 62 nM). Screening hit, compound **2**, showed more modest inhibition of PKD (IC_{50} = 321 nM) and HDAC nuclear export (IC_{50} = 5420 nM). Like **1**, compound **2** did not achieve the desired selectivity vs a subset of the PKC isoforms. Rather, **2** exhibited 10-fold inverted selectivity vs PKCδ (IC_{50} = 20 nM). Further, owing to the role of PKC in PKD activation, the cellular activities of **1** and **2** cannot be firmly attributed to PKD inhibition. That is, HDAC nuclear export activity of **1** and **2** cannot rule out the contribution of direct and exclusive PKC inhibition.

Compound **10b** highlights the sensitivity of the 1-naphthyridine substituent for PKD, PKCα, and PKCδ activity. Compound **13a** hinted that introduction of a 2-pyridine substituent benefited PKD activity without enhancing PKC inhibition. The piperazine **11** gained 5-fold PKD activity vs the parent ethylenediamine **2**. Combining the piperazine with the 2-pyridine substituent, as with **12c** (IC_{50} = 50 nM) or **13c** (IC_{50} = 0.6 nM), afforded potent PKD inhibitors with useful (20- to 1400-fold) selectivity vs PKCs. Similarly weak PKC activity was observed for all subsequent compounds bearing 2-pyridyl substituents described throughout the present study. Encouragingly, the cellular activity of **13c** (IC_{50} = 32 nM) was more potent than could be expected for micromolar inhibition across PKC isoforms. With simple substitution changes, naphthyridine **13c** reflects a ~500-fold increase in target activity and a ~15,000-fold increase in PKD vs PKCδ selectivity relative to the hit compound **2**.

In Figure 2, a possible binding mode for **13c** in the ATP-binding site of PKD1 is shown, wherein the alkylaminopyridine forms two hydrogen-bonding contacts with the Leu662 hinge residue, the naphthyridine 6-nitrogen contacts the catalytic Lys612, and the piperazine nitrogen participates in a salt bridge with a pendent Glu710 of the sugar pocket. However, the pseudosymmetry of the series renders the 6-naphthyridine nitrogen of **13c** a viable alternative for the hinge contact and the pyridine a viable alternative contact for the catalytic Lys. If indeed the binding mode depicted in Figure 2 is accurate and a similar orientation is realized for PKC, the intolerance of PKCs for the 2-pyridyl substituent may come from steric clash with the residues adjacent to the hinge, which are uniformly larger (Phe or Tyr) for the PKCs, where the PKDs contain the more flexible Lys. In the absence of X-ray crystallographic data for a representative naphthyridine inhibitor in PKD and PKC, a specific structural basis for the observed selectivity impact with substitution of the pyridine is unknown.

To better understand the contribution of the core 2,6-naphthyridine to the PKD activity, the team explored modification of the 6-naphthyridine nitrogen, while keeping the "2"-naphthyridine nitrogen constant (Table 2). Of the compounds in Table 2, only the isoquinoline **22a**, 2,5-naphthyridine **22d**, and quinazoline **22e** achieved IC_{50}s less than 50 nM. In no case where the 6-nitrogen was deleted or relocated did the PKD activity match that of the parent **13c**. These results are consistent with the function of the 6-nitrogen as a hydrogen-bond acceptor to the enzyme.

In certain cases, modulating the bulkiness, basicity, and/or polarity of amine-containing compounds can improve drug-like qualities. The compounds indicated in Table 3 were

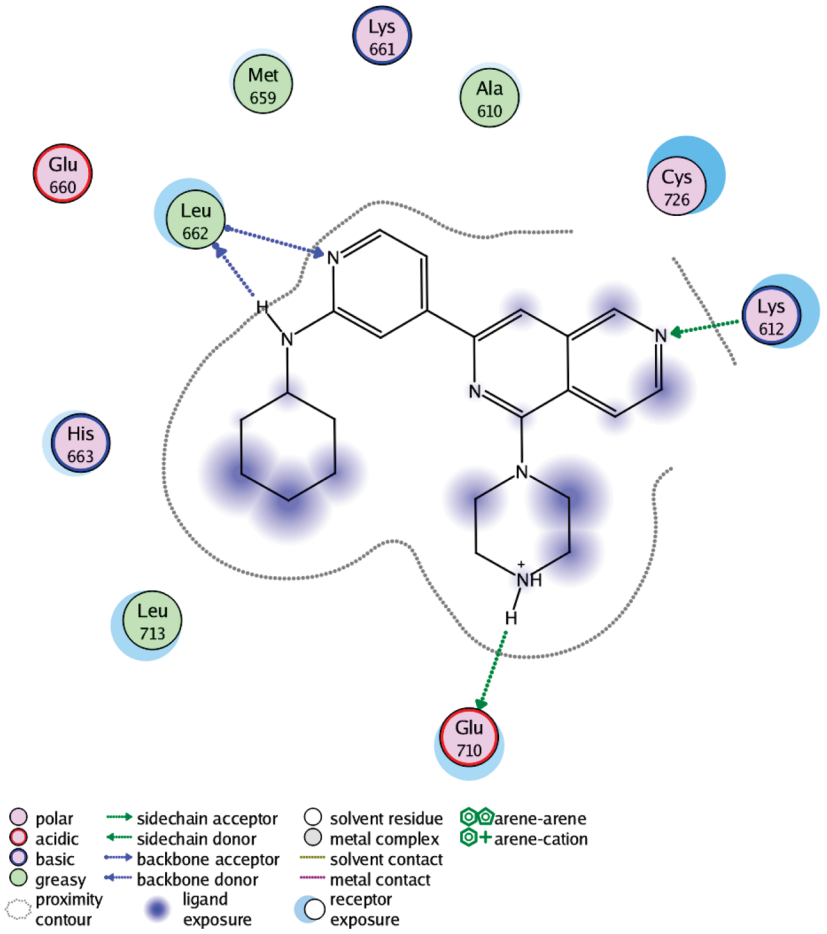

Figure 2. Proposed key contacts for PKD inhibitor **13c** in PKD1.

Table 2. Naphthyridine Core Modifications

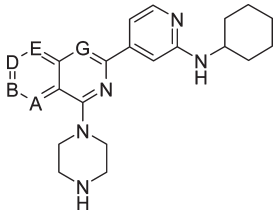

						IC_{50} (nM)	
compd	A	B	D	E	G	PKD1	HDAC exptl
22a	CH	CH	CH	CH	CH	12	356
22b	N	CH	CH	CH	CH	695	> 10000
22c	CH	N	CH	CH	CH	191	1558
22d	CH	CH	CH	N	CH	15	262
22e	CH	CH	CH	CH	N	43	1521

prepared to explore the effects of amine branching and basicity on PKD potency. This series highlights the flat SAR with respect to PKD and HDAC export, with only the weakest base **13l** falling 10-fold outside the IC_{50} of the parent **13c**. Replacing the cyclohexyl with an alternative but neutral branched aliphatic group with greater polarity (e.g., THP) gave compounds **13f** and **13g**. The calculated log *P* values for **13c** and **13f** are significantly different (4.12 for **13c** and 1.72 for **13f**), yet compounds **13f** and **13g** showed equal potency relative to their cyclohexyl comparators **13c** and **13d**. Although the piperazine likely contributes to the high aqueous solubility at pH 6.8 of both **13c** (734 μM) and **13f** (887 μM), the flexibility to introduce pyridine 2-substituents with greater polarity, like the aminoTHP, can provide a potentially useful mechanism to modify the physical properties (e.g., aqueous solubility) or the off-target profile of naphthyridine analogues.

A second study of the 1-naphthyridine substituent carried either the cyclohexylamino or 4-tetrahydropyranamino findings of the above (Table 4). As with the entries of Table 1, untethered alcohols, such as **13n**, offered modest PKD inhibition, while introdution of a ring enhanced activity (**13j**, IC_{50} = 15 nM). Building from the piperazine, the first amides **13o** and **13m** were disappointing, especially with respect to cellular activity. Reinserting a basic nitrogen, as with **13r**, enhanced the PKD and cellular activity relative to **13m**. Thereafter, the team was pleased to identify the piperidine carboxamide series, including **13s** and **13t**, which offered good PKD inhibition and cellular activity in the absence of a basic nitrogen. Bulkier analogues, such as **13y** and **13z**, exhibited low nanomolar IC_{50}s vs PKD but 10-fold weaker HDAC export activity compared to the most potent examples. Again, in cases such as **13ae** and **13v**, where a pendent base was (re)installed, the cellular activity (IC_{50} values of 44 and 25 nM, respectively) matched that of piperazine **13c** (IC_{50} = 32 nM).

Further comparison of prototype PKD inhibitors amine **13c** and amide **13y** in vitro, in cells, and in vivo follows. In vitro (Figure 3), compounds **13c** and **13y** dose-dependently inhibited autophosphorylation of recombinant human PKD1

Table 3. 1-Naphthyridine Modifications: Piperazines and Aminopiperidine

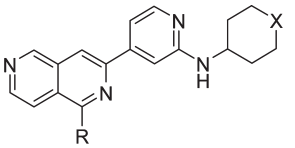

Cpd	X	R	IC_{50} (nM) PKD1	IC_{50} (nM) HDAC exp
13h	CH_2	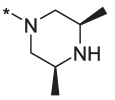	3	30
13i	CH_2	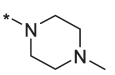	2	206
13d	CH_2	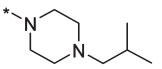	6	299
13k	CH_2	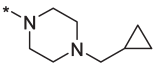	2	221
13l	CH_2	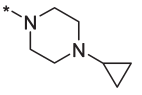	13	454
13q	CH_2	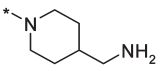	1	49
13f	O	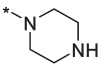	0.4	10
13g	O	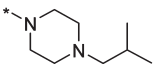	1	78

(Ser916) and PKD2 (Ser867). At concentrations as low as 10 nM, **13c** partially blunted PKD1 autophosphorylation and nearly completely blunted PKD2 autophosphorylation in the absence of the HDAC peptide, a 25-mer substrate peptide designed to model one of the HDAC serine residues (Ser498) that is phosphorylated by PKD.[21]

For compound **13y**, partial control of PKD1 autophosphorylation was observed at 10 nM, with near complete inhibition at 100 nM. However, 100 nM of **13y** was needed to block PKD2 autophosphorylation. These experiments compared well with the relative and absolute biochemical assay results for **13c** and **13y** (PKD1 data from Tables 1 and 3, PKD2 IC_{50} values of 2 and 16 nM, respectively) and confirmed the pan-PKD inhibitory activity of the 2,6-naphthyridine series with an alternative substrate. Lastly, inhibition of both PKDs by **13c** and **13y** occurred in the presence of an HDAC5 peptide, which served as a surrogate for the native, full length HDAC5 present in cells.

GPCR agonists, such as prostaglandin F2α (PGF2α) utilized in the HDAC export assay or phenylephrine (PE) and endothelin-1 (ET-1) utilized for Figure 4 below, initiate cell surface-signaling to PKC and consequent activation of PKD to drive GFP-HDAC5 export to the cytosol of rat cardiac myocytes (top row, Figure 4). In addition, direct stimulation of PKC with the phorbol ester PMA causes nuclear export of GFP-HDAC5. With all stimuli shown to cause export of GFP-HDAC5, pretreatment of the cells with 1 μM **13c** controlled GFP-HDAC5 nuclear export, consistent with the hypothesis that PKD integrates multiple signals originating at the cell surface.

In PE-stimulated rat cardiac myocytes (Figure 5), **13c** and **13y** dose-dependently block PKD activity. PKD activity, which is gauged by both autophosphorylation (Ser916) and phosphorylation of the substrate HDAC5 (Ser498), occurred without loss of PKD activation (PKC-mediated phosphorylation at Ser744/748 not shown). Consistent with the HDAC export assay that tracks PGF2α-driven nuclear export of superphysiologic GFP-HDAC, both **13c** and **13y** blocked phosphorylation of GFP-HDAC5 (Ser498) at 1000 nM. Additionally, the relative potency between **13c** (IC_{50} = 32 nM) and **13y** (IC_{50} = 391 nM) in the HDAC export assay is reflected in the ability of 100 nM **13c**, but not **13y**, to normalize pHDAC to baseline. As well, both compounds dose-dependently inhibited native PKD autophosphorylation, albeit at concentrations higher than those required to block pHDAC. For example, at a dose 10-fold greater than that which successfully controlled pHDAC, residual pPKD was detected in the presence of 1000 nM **13c** by comparison to pPKD in unstimulated cells. This phenomenon was matched throughout the present study. That is, we routinely observed inhibition of pHDAC in isolated cardiac myocytes at lower concentrations than those required to blunt autophosphorylation of native PKD.

Further profiling of **13c** and **13y** supported their use as prototype PKD inhibitors for in vivo study. In male Sprague−Dawley rats, the pharmacokinetic parameters of **13c** and **13y** were evaluated following administration as solutions (Table 5).

Table 4. 1-Naphthyridine Modifications: Alcohols and Amides

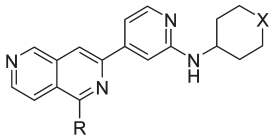

			IC_{50} (nM)	
Cpd	X	R	PKD1	HDAC exp
13n	CH_2	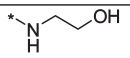	382	>1000
13j	CH_2	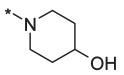	15	474
13o	CH_2	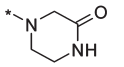	4931	>>1000
13m	CH_2	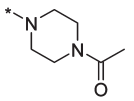	19	>1000
13s	CH_2	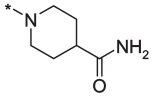	83	204
13u	CH_2	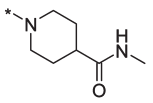	3	94
13ae	CH_2	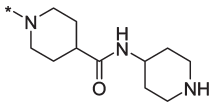	1	44
13v	CH_2	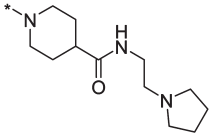	1	35
13w	CH_2	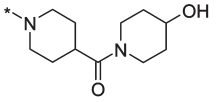	4	294
13r	O	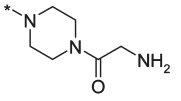	5	749
13t	O	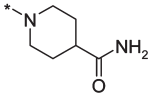	2	20
13x	O	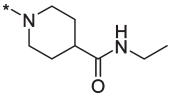	3	83
13y	O	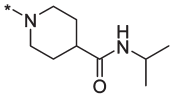	3	391
13z	O	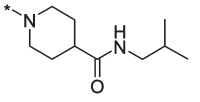	2	228
13ac	O	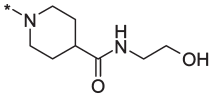	2	60
13aa	O	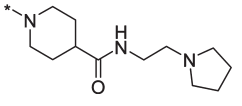	1	96

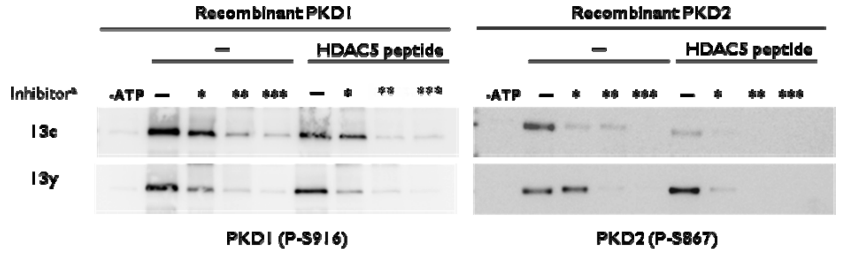

Figure 3. PKD inhibitors **13c** and **13y** block in vitro autophosphorylation of PKD1 (Ser916) and PKD2 (Ser867) in the absence or presence of an HDAC5 peptide. The concentrations at which PKD autophosphorylation is inhibited are consistent with the IC_{50} values in the PKD biochemical assays: (a) (−) 0 μM, (∗) 0.01 μM, (∗∗) 0.1 μM, (∗∗∗) 1 μM compound concentration.

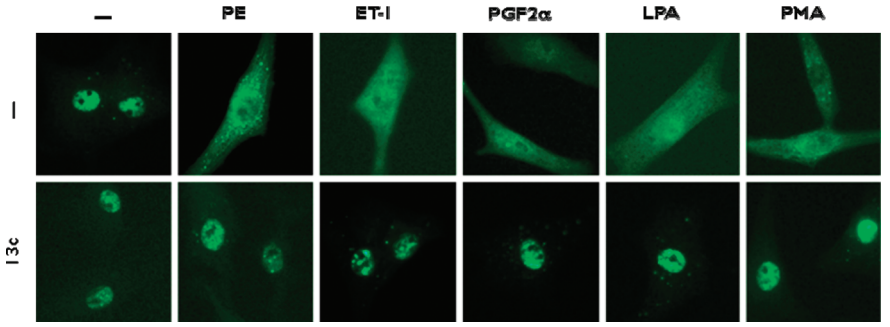

Figure 4. In neonatal rat ventricular myocytes (NRVMs), 1 μM **13c** blocks GFP-HDAC5 nuclear export in response to a variety of stimuli, including 10 μM phenylephrine (PE), endothelin-1 (ET-1), prostaglandin F2α (PGF2α), lysophosphatidic acid (LPA), or phorbol 12-myristate 13-acetate (PMA).

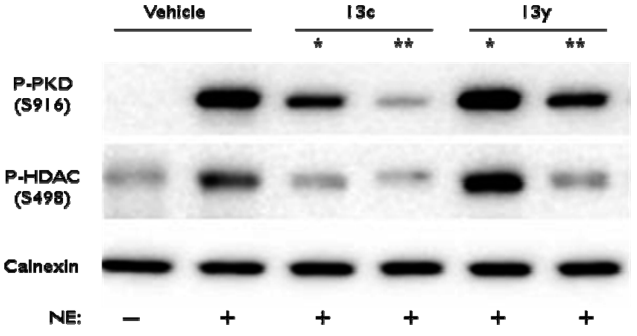

Figure 5. In NRVMs, compound **13c** and **13y** block PE-stimulated PKD activity. In accordance with their relative and absolute potencies in the HDAC export assay, compounds **13c** (at 0.1 and 1 μM) and **13y** (at 1 μM) block phosphorylation of the PKD substrate HDAC (pSer498). At 1 μM, **13c** effectively blocks PKD autophosphorylation (pSer916) while **13y** produces partial reduction: (a) (−) 0 μM, (∗) 0.1 μM, (∗∗) 1 μM compound concentration.

To accommodate the low aqueous solubility of **13y** for iv administration, an NMP and Cremophor EL containing vehicle was used for the determination of PK properties. For consistency, the vehicle used for **13c** to determine PK parameters was matched to that used for **13y**. For the subsequent high dose exposure and efficacy studies in rats, both **13c** and **13y** were administered orally as suspensions in methylcellulose or subcutaneously in acidified captisol. Following an iv dose, **13c** was cleared rapidly from the plasma and showed a large volume of distribution (12 L/kg) that was significantly greater than the total body water in rats. When administered as a solution via oral gavage, **13c** was rapidly absorbed with a low absolute oral bioavailability of 4%. A subset of the amides, including **13y**, showed measurable plasma exposure following oral administration, with C_{max}, $AUC_{0\text{-}8h}$, and bioavailability exceeding those of the piperazine **13c** (Table 5). A 50 mg/kg po dose of compounds **13c** and **13y** as suspensions to the DSS rat produced higher plasma exposures and similar plasma curve shapes relative to the low-dose po studies above (Figure 6). Compound **13c** for its potency and consistent plasma exposure and high cardiac exposure (not shown) and the amide **13y** for its different plasma PK profile, improved kinase

Table 5. Pharmacokinetic Profile of **13c** and **13y**[a]

PK parameter	**13c**	**13y**
dose iv/po (mg/kg)	2/5	2/5
po C_{max} (nM)	128 ± 29	466 ± 535
po T_{max} (h)	0.25 ± 0.1	0.5
po AUC_{0-8h} (nM·h)	193 ± 175	633 ± 647
iv AUC_{0-8h} (nM·h)	1923 ± 460	1107 ± 313
CL ((mL/min)/kg)	32 ± 12	61 ± 19
V_{ss} (L/kg)	12 ± 1	7.0 ± 7.8
T_{half} (h)	5.2 ± 1.9	5.4 ± 4.4
bioavailability (%)	4	23

[a] AUC_{0-8h} reported here, not AUC_{∞}.

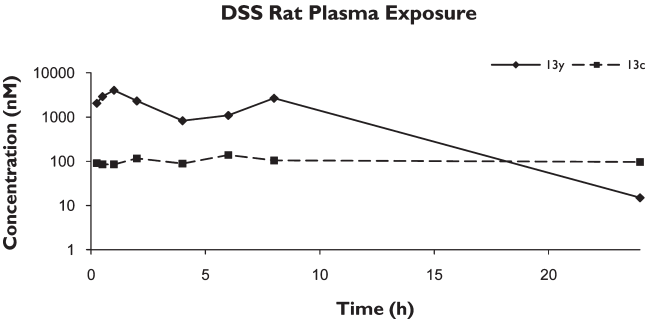

Figure 6. DSS rat plasma exposure following 50 mg/kg oral administration of **13c** and **13y** as a suspension in 0.5% methylcellulose and 0.5% Tween-80.

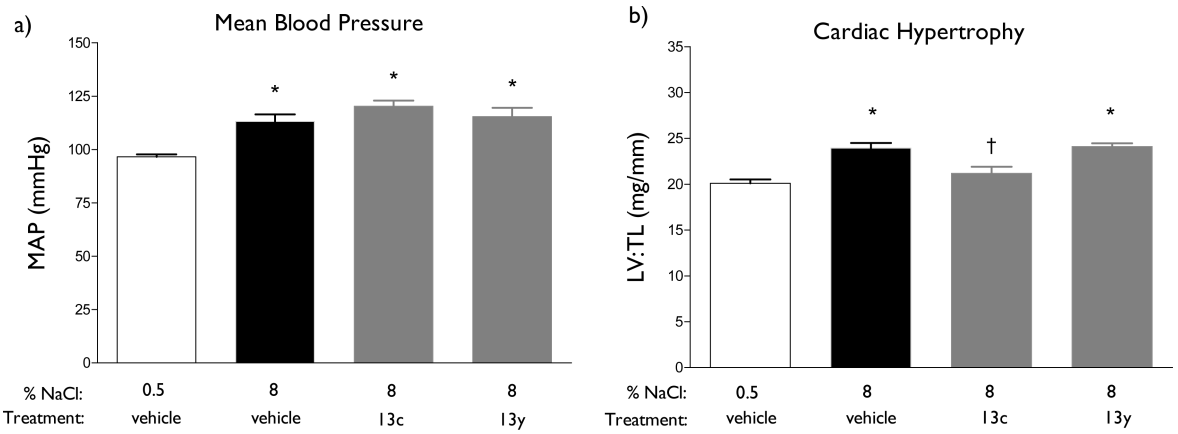

Figure 7. Effect of compound **13c** and **13y** given 50 (mg/kg)/day po as a suspension in methylcellulose for 14 days in the DSS rat on (a) mean blood pressure and (b) cardiac hypertrophy (left ventricular mass/tibia length) on day 14. Neither compound attenuated the increase in mean blood pressure observed with high (8%) salt diet. Compound **13c**, but not **13y**, blunted high-salt-induced cardiac hypertrophy (LV/TL): (∗) $p <$ 0.05 vs 0.05% NaCl plus vehicle; (†) $p < 0.05$ vs 8% NaCl plus vehicle.

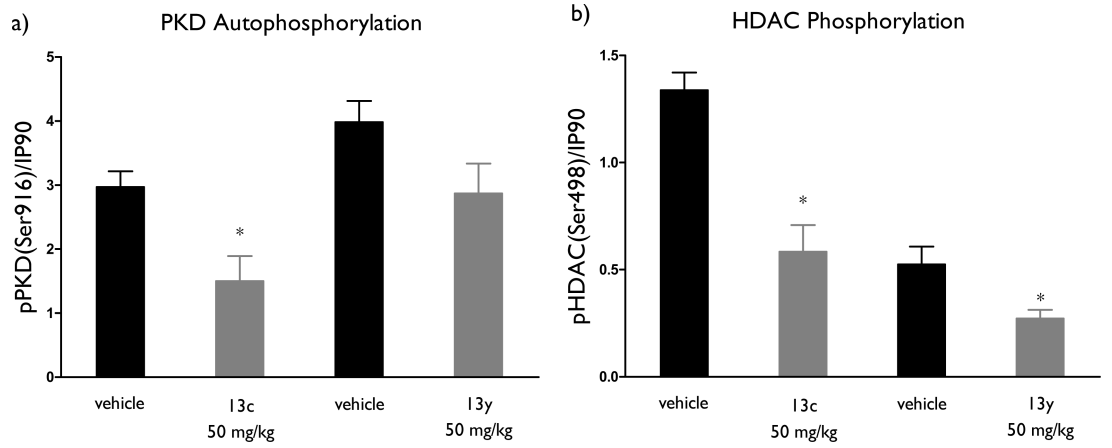

Figure 8. Biomarker readout in the DSS rat in a surrogate cell type on day 14. In peripheral blood mononuclear cells (PBMCs), PMA-stimulated, (a) autophosphorylation of PKD at Ser916 is blunted by compound **13c** and (b) phosphorylation of the PKD substrate HDAC at Ser498 is blunted by both **13c** and **13y** relative to the vehicle control: (∗) $p < 0.05$ vs vehicle.

Table 6. Percent Activity Remaining in the Presence of 1 μM **13c** or **13y** vs Set of PKD Family Member Kinases and IC_{50} Values versus Adrenergic Receptors

	activity (%)	
kinase	**13c**	**13y**
PKD1	2	3
PKD2	2	7
GSK3β	3	38
CaMKIδ	67	100
CaMKIIβ	13	73
CaMKIIγ	26	96
CaMKIIδ	45	91
CaMKIV	100	100
MARK1	28	80
SIK1	86	99
GRK5	100	100
PKCδ	78	100
PKCε	72	80
	IC_{50} (nM)	
receptor	**13c**	**13y**
α1AR	7202	> 10000
β1AR	2351	> 10000

selectivity, and spotless receptor binding profile (Table 6) were investigated in the in vivo hypertrophy models.

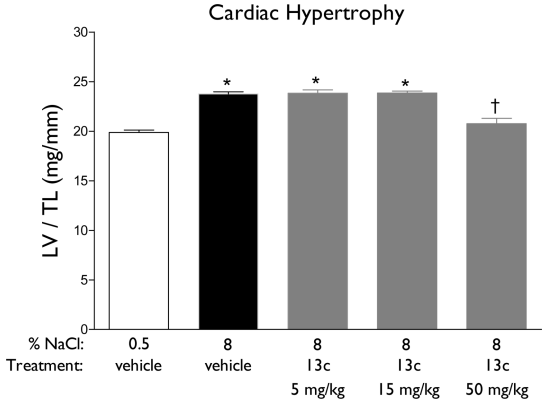

Figure 9. Effect of compound **13c** given 5, 10, and 50 (mg/kg)/day po as a suspension in methylcellulose on day 14 of 14 days in the DSS rat on cardiac hypertrophy (left ventricular mass/tibia length). Only the 50 mg/kg po dose attenuates high-salt-diet-induced cardiac hypertrophy (LV/TL): (∗) $p < 0.05$ vs 0.05% NaCl plus vehicle; (†) $p < 0.05$ vs 8% NaCl plus vehicle.

Compound **13c** or **13y** were adminstered at 50 (mg/kg)/day po for 14 days to DSS rats concomitantly with a switch to a high-salt (8%) diet. Control animals remaining on normal-salt diet (0.5%) or on high-salt (8%) diet were administered

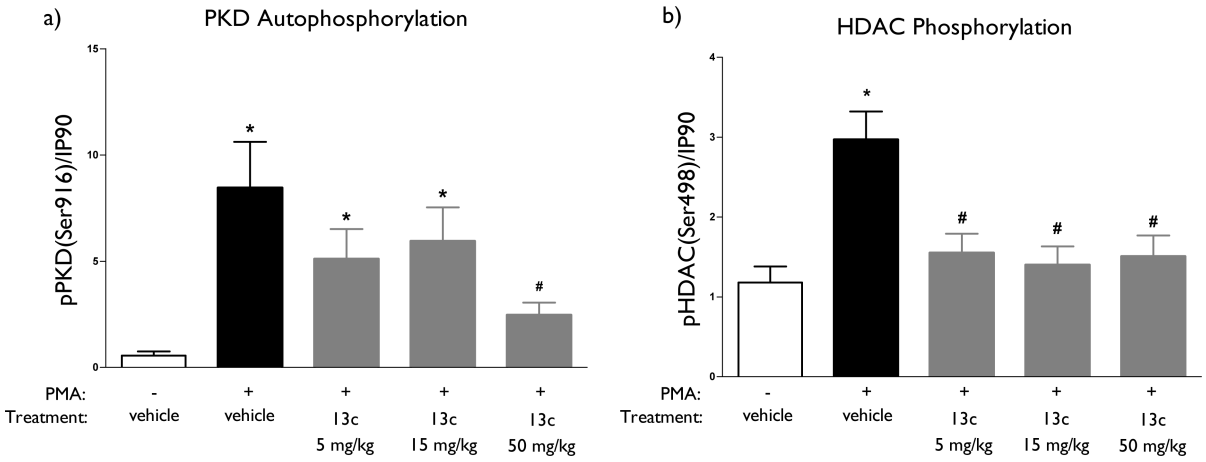

Figure 10. Biomarker readout in the DSS rat in a surrogate cell type on day 14. In peripheral blood mononuclear cells (PBMCs), PMA-stimulated, (a) autophosphorylation of PKD at Ser916 is blunted by the highest dose of compound **13c** and (b) phosphorylation of the PKD substrate HDAC at Ser498 is reduced by all compound doses: (*) $p < 0.05$ vs vehicle; (#) $p < 0.05$ vs vehicle plus PMA.

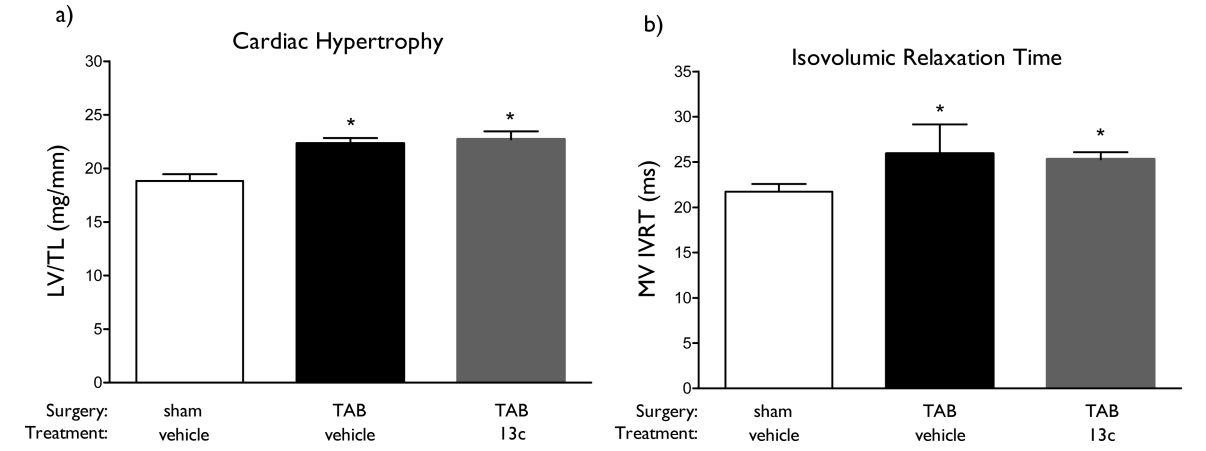

Figure 11. Effect of compound **13c** given 15 (mg/kg)/day sc in acidified captisol in the thoracic aortic banded (TAB) rat on (a) cardiac hypertrophy (left ventricular mass/tibia length) and (b) a marker of diastolic function isovolumic relaxation time (IVRT) on day 14. Neither parameter is affected by compound treatment: (*) $p < 0.05$ vs vehicle.

vehicle daily. As anticipated, vehicle-treated animals on high-salt diet exhibited hypertension, or elevated mean arterial pressure (MAP), and hypertension-driven cardiac hypertrophy relative to the vehicle-treated rats on normal-salt diet (Figure 7). The mass of the left ventricle (LV) normalized to the animal size by the tibia length (TL) gives the index of cardiac hypertrophy. After 14 days, rats given a high-salt diet exhibited a consistently elevated mean blood pressure (Figure 7a) and a corresponding ~20% increase in the LV/TL relative to the normal-salt rats (Figure 7b). While neither compound **13c** nor **13y** blocked high-salt induced hypertension (Figure 7a), the compounds were differentiated with respect to cardiac hypertrophy. Compound **13c**, but not **13y**, gave a statistically significant reduction in the LV/TL (Figure 7b). In the absence of changes to MAP, the antihypertrophic behavior of **13c** at 50 (mg/kg)/day po cannot be attributed to simple relief of hypertension.

To circumvent technical difficulties with monitoring phosphorylation state changes to the modestly abundant HDAC5 in intact rat hearts, the team devised an ex vivo assay to monitor PKD inhibition in a surrogate cell type, the peripheral blood mononuclear cells (PBMCs). As with the cardiac myocytes of Figure 4, PKD was activated in PBMCs by treatment with phorbol ester (PMA). In PMA-stimulated PBMCs taken from the DSS study above (Figure 8), both compounds **13c** and **13y** reduced the substrate HDAC phosphorylation, but only the efficacious **13c** also reduced PKD autophosphorylation. A dose−response study conducted with **13c** given 50, 15, or 5 (mg/kg)/day in the DSS rat (Figure 9) confirmed the antihypertrophic response at the 50 (mg/kg)/day dose as above (Figure 7b). However, while the lower doses of 15 and 5 (mg/kg)/day achieved 6700 and 1000 nM cardiac exposures, respectively, neither compound attenuated high salt-induced cardiac hypertrophy. From the PKD activity biomarkers observed in PBMCs (Figure 10), all three doses of **13c** blunt pHDAC, but only the highest 50 mg/kg dose achieves a statistically significant reduction of PKD autophosphorylation.

To follow up on the observation that $PKD1^{-/-}$ limits the pressure-overload-induced cardiac hypertrophy observed in the TAB rat, compound **13c** was evaluated in a rat TAB model. In this case, surgical banding of the thoracic aorta was completed prior to compound administration. Compound was administered parenterally (15 (mg/kg)/day sc) 1 day postsurgery to limit the postsurgical stress observed with oral gavage. On day 14, 2 h after administration of the final oral dose, plasma and cardiac exposures (~60000 nM) closely matched those observed at the same time in the DSS rat study

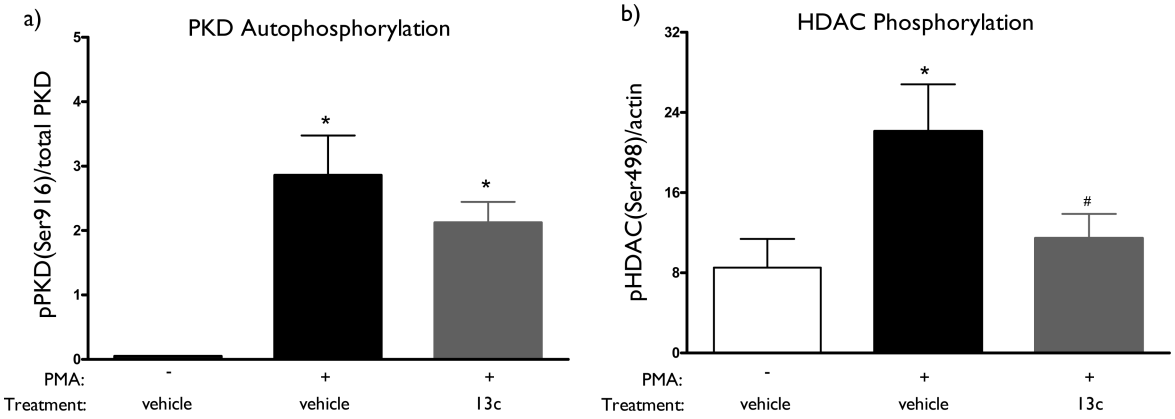

Figure 12. Biomarker readout in the TAB rat in a surrogate cell type on day 14. In PBMCs, PMA-stimulated, (a) autophosphorylation of PKD at Ser916 with compound **13c** treatment is not significantly different from vehicle control and (b) phosphorylation of the PKD substrate HDAC at Ser498 is normalized to baseline levels: (*) $p < 0.05$ vs vehicle; (#) $p < 0.05$ vs vehicle plus PMA.

Table 7. **13c** and **13y** Exposures in DSS Rat Plasma and Left Ventricle 2 h after Final Dose on Day 14

compd	rat model	dose ((mg/kg)/day)	route	in plasma (nM)	in left ventricle (nM)
13c	DSS	50	po	541 ± 99	59681 ± 16330
	DSS	15	po	305 ± 155	6687 ± 3084
	DSS	5	po	87 ± 42	1001 ± 521
	TAB	15	sc	288 ± 111	60992 ± 14860
13y	DSS	50	po	1653 ± 1046	2021 ± 1139

(Table 7). Unfortunately, compound **13c** in the TAB rat had no effect on cardiac hypertrophy (LV/TL) in the TAB rat (Figure 11), in direct contrast to the efficacy observed in the DSS rat and the reported results with PKD1 knockout in the mouse TAB model. Neither did **13c** affect cardiac function, as gauged by the accepted marker of diastolic dysfunction, isovolumic relaxation time (IVRT). In this case, the biomarker readout in the PBMCs indicated significant blunting of pHDAC without statistically significant control of PKD autophosphorylation (Figure 12).

Conclusions

Starting from a dual PKC/PKD inhibitor identified by HTS, potent prototype pan-PKD inhibitors were identified with useful selectivity vs representative upstream PKD-activating PKC isoforms (> 1000-fold). Further, compounds **13c** and **13y** were well-tolerated by daily po or sc administration up to 2 weeks in rat models of heart failure with micromolar cardiac tissue exposures above the cellular IC_{50}.

In vivo, the most potent but overall less selective (vs a broad kinome and receptor panel) inhibitor **13c** (PKD1 IC_{50} = 0.6 nM, HDAC export IC_{50} = 32 nM) demonstrated efficacy at the 50 mg/kg po dose in the DSS rat model but not at the 15 mg/kg sc dose in the TAB rat model. Although the doses and routes of administration were different (necessitated for technical reasons), the plasma (288−541 nM) and cardiac (~60000 nM) exposures of **13c** were matched between the two studies. In both animal models, inhibitor **13c** blunted PMA-stimulated phosphorylation of the PKD substrate HDAC in a surrogate cell type (PBMCs). Therefore, the same exposure of **13c** and consequent control of pHDAC produced model-dependent effects on cardiac hypertrophy. Further, the TAB rat, which was anticipated to be the best model of PKD inhibition based on the PKD1 knockout studies in the TAB mouse, provided a second disconnect with the expected in vivo cardiac profile of a PKD inhibitor. The lack of efficacy in the TAB rat with **13c** represents a point of difference with the observed protection afforded by PKD1 knockout in the TAB mouse.

Because of the high cardiac exposure together with the off-target profile, the efficacy of **13c** in the DSS rat at 50 mg/kg cannot be firmly ascribed to PKD inhibition. Inhibition of an alternative kinase or antagonism of an upstream receptor is also consistent with the observed result. For example, either α-[22] or β-adrenergic[23] receptor blockade (**13c** β1AR IC_{50} = 2351 nM, antagonist) controls high salt-induced cardiac hypertrophy in the DSS rat at subantihypertensive doses. Further, lower doses of **13c** (15 or 5 (mg/kg)/day) maintained 6700 and 1000 nM cardiac exposures in the DSS rat, respectively, well in excess of the cellular HDAC export IC_{50} in isolated rat cardiac myocytes. Therefore, even the lowest observed cardiac exposure of **13c** exceeds the effective concentration in the myocytes by more than an order of magnitude. While these exposures are likely to produce pharmacologic inhibition of the PKDs, the strongest evidence of PKD inhibition comes from the corroborating biomarker evidence.

In addition to the availability of the compounds in the target organ, biomarker evidence generated from PBMCs isolated from the in vivo model affords a direct measure of pharmacologic PKD inhibition. Most importantly, all doses of **13c** blunted PMA-stimulated phosphorylation of native HDAC in the PBMCs. The coupling of the micromolar concentrations in cardiac tissue to the biomarker PBMC data is consistent with pharmacological inhibition of the target in the heart at all three doses of **13c**. Likewise, a second PKD inhibitor, **13y**, which exhibits limited receptor affinity and higher kinase selectivity vs a set of putative HDAC kinases, reached micromolar concentrations in cardiac tissue and blunted PMA-stimulated HDAC phosphorylation in the PBMCs, again in the absence of an effect on cardiac hypertrophy in the DSS rat. Therefore, in contrast to the target hypothesis, no direct correlation between pHDAC levels and cardiac hypertrophy was observed. That is, the reduced HDAC phosphorylation observed in the PBMCs with both test compounds at all test doses was not linked to control of high salt-induced cardiac hypertrophy in the DSS rat. If (1) the cardiac exposure of **13c** and **13y** and the pHDAC reduction observed in the PBMCs accurately model reduced cardiac pHDAC levels and (2) the DSS and TAB rat models accurately predict clinical success for PKD inhibitors as

antihypertrophic agents for the treatment of heart failure, then the in vivo responses of compounds **13c** and **13y** separate control of cardiac pHDAC with therapeutic potential in heart failure.

In the rodent cardiac hypertrophy model studies, PKD inhibition may not be functionally equivalent to loss of PKD1. A possible rationale lies in the protocol differences between the relevant rat and mouse TAB experiments. That is, loss of PKD1 is complete and consistent over the course of the experiment where PKD inhibition is initiated postsurgery and potentially variable. Alternatively, HDAC may represent only one of multiple relevant PKD substrates. For example, in the DSS rat model, the only case in which blockade of PKD autophosphorylation was statistically significant, in vivo antihypertrophic activity was also observed (50 (mg/kg)/day **13c** in the DSS rat). While inconsistent with the target hypothesis of pHDAC/MEF2 signaling, failure to completely block phosphorylation of multiple PKD substrates (e.g., HDAC and PKD itself) could account for the disconnect between PKD inhibition and PKD1 knockout in banded rodents.

On the basis of potency, tissue exposure, and biomarker evidence, the aggregate data support that the prototype PKD inhibitors **13c** and **13y** were able to block phosphorylation and nuclear export of the MEF2 repressor HDAC in the target tissue in vivo. Still, the moderate kinase selectivity of the naphthyridine PKD inhibitors (especially **13c**) complicates interpretation of the hypertrophic response (or lack thereof) in both models, since pleiotropic effects (e.g., inhibition of an antihypertrophic kinase such as GSK3β[24]) cannot be ruled out. To shed further light on this question, the identification and in vivo profiling of exquisitely potent pan-PKD inhibitors with enhanced selectivity vs a broad kinase panel are reported in the following paper.[25] Taken in combination with the present study, in vivo results from the second chemotype were utilized to investigate further the therapeutic potential of PKD inhibition as an antihypertrophic target.

Experimental Section

PKD1 Assay. The assay to measure protein kinase D1 (PKD1) activity was a time-resolved fluorescence resonance energy transfer (TR-FRET) assay using PerkinElmer's LANCE technology. In this case, a biotinylated syntide-2 peptide (with sequence PLARTLSVAGLPGKK) was used as the substrate in this reaction. Phosphorylation of the syntide-2 substrate (at the serine residue) was detected by a specific antibody that recognizes the phosphorylated peptide and a europium labeled secondary antibody. A second fluorophore, allophycocyanin (APC), was conjugated to streptavidin that binds the biotinylated syntide-2 peptide. For detection, the europium fluorophore can be excited by 340 nm light which then emits at 615 nm. Therefore, when the europium labeled secondary antibody binds on the phosphorylated peptide, it is brought into close contact with the APC and excites this fluorophore. The APC emission is at 665 nm, and the (665 nm)/(615 nm) ratio is a readout of PKD1 activity. This assay was performed with full length wild-type enzyme that is expressed and purified from Sf9 insect cells. The reaction buffer consists of 35 mM Tris-HCl, pH7.5, 5 mM $MgCl_2$, 0.02% Tween-20, 20 μM ATP, 1 mM DTT, and 0.2 μg/mL PKD1 enzyme. The enzyme reaction was initiated by the addition of 2 μM syntide-2 peptide substrate and the reaction carried out for 50 min at room temperature. The reaction was stopped by a stop/detection buffer consisting of 50 mM EDTA, 0.18 mg/mL rabbit polyclonal anti-phospho syntide-2 antibody, 0.5 nM europium labeled anti-rabbit IgG, and 10 nM streptavidin conjugated APC. After a 1 h incubation with the stop/detection buffer, the reaction was read on an Envision 2100 reader using a LANCE Eu/APC dual protocol. As described above, a (665 nm)/(615 nm) ratio was determined to measure substrate phosphorylation and enzyme activity. Compounds are typically tested in an 11-point dose response fashion in triplicate for each concentration used. IC_{50} values are calculated using an activity base (IDBS) software program.

PKD2 Assay. The assay to measure protein kinase D2 (PKD2) activity was a time-resolved fluorescence resonance energy transfer (TR-FRET) assay using PerkinElmer's LANCE technology. In this case, a biotinylated syntide-2 peptide was used as the substrate in this reaction. Phosphorylation of the syntide-2 substrate was detected by a specific antibody that recognizes the phosphorylated peptide. A second fluorophore, APC, was conjugated to streptavidin that binds the biotinylated syntide-2 peptide. For detection, the europium fluorophore can be excited by 340 nm light which then emits at 615 nm. Therefore, when the europium labeled secondary antibody binds on the phosphorylated peptide, it was brought into close contact with the APC and excites this fluorophore. The APC emission was at 665 nm, and the (665 nm)/(615 nm) ratio was a readout of PKD2 activity.

The assay was performed with full length wild-type enzyme purchase from Invitrogen. The reaction buffer consists of 35 mM Tris-HCl, pH7.5, 5 mM $MgCl_2$, 0.02% Tween-20, 20 μM ATP, 1 mM DTT, and 0.2 μg/mL PKD2 enzyme. The enzyme reaction was initiated by the addition of 2 μM syntide-2 peptide substrate and the reaction carried out for 50 min at room temperature. The reaction was stopped by a stop/detection buffer consisting of 50 mM EDTA, 0.18 mg/mL rabbit polyclonal anti-phospho syntide-2 antibody, 0.5 nM europium labeled anti-rabbit IgG, and 10 nM streptavidin conjugated APC. After a 1 h incubation with the stop/detection buffer, the reaction was read on an Envision 2100 reader using a LANCE Eu/APC dual protocol. As described above, a (665 nm)/(615 nm) ratio was determined to measure substrate phosphorylation and enzyme activity. Compounds are typically tested in an 11-point dose response fashion in triplicate for each concentration used. IC_{50} values are calculated using an activity base (IDBS) software program.

PKD3 Assay. The assay to measure protein kinase D3 (PKD3) activity was a time-resolved fluorescence resonance energy transfer (TR-FRET) assay using PerkinElmer's LANCE technology. In this case, a biotinylated syntide-2 peptide was used as the substrate in this reaction. Phosphorylation of the syntide-2 substrate was detected by a specific antibody that recognizes the phosphorylated peptide. A second fluorophore, APC, was conjugated to streptavidin that binds the biotinylated syntide-2 peptide. For detection, the europium fluorophore can be excited by 340 nM light which then emits at 615 nm. Therefore, when the europium labeled secondary antibody binds on the phosphorylated peptide, it was brought into close contact with the APC and excites this fluorophore. The APC emission was at 665 nm, and the (665 nm)/(615 nm) ratio was a readout of PKD3 activity.

PKC Assays. The compounds of the invention are tested for their activity on different PKC isotypes according to the following method. Assay was performed in a white with clear bottom 384-well microtiter plate with nonbinding surface. The reaction mixture (25 μL) contains 1.5 μM tridecapeptide acceptor substrate that mimics the pseudo substrate sequence of PKCα with the Ala $\rightarrow$ Ser replacement, 10 μM ^{33}P-ATP, 10 mM $Mg(NO_3)_2$, 0.2 mM $CaCl_2$, PKC at a protein concentration varying from 25 to 400 ng/mL (depending on the isotype used), lipid vesicles (containing 30 mol % phosphatidylserine, 5 mol % DAG, and 65 mol % phosphatidylcholine) at a final lipid concentration of 0.5 mM, in 20 mM Tris-HCl buffer, pH 7.4, and 0.1% BSA. Incubation was performed for 60 min at room temperature. Reaction was stopped by adding 50 μL of stop mix (100 mM EDTA, 200 μM ATP, 0.1% Triton X-100, 0.375 mg/well streptavidin-coated SPA beads in phosphate buffered saline

without Ca, Mg. After 10 min of incubation at room temperature, the suspension was spun down for 10 min at 300*g*. Incorporated radioactivity was measured in a Trilux counter for 1 min. IC_{50} measurement was performed on a routine basis by incubating a serial dilution of inhibitor at concentrations ranging between 1 and 1000 nM. IC_{50} values are calculated from the graph by curve fitting with XL fit software. Human recombinant PKCα was obtained from Oxford Biomedical Research and was used under the assay conditions as described above. Human recombinant PKCδ was obtained from Oxford Biomedical Research and was used under the assay conditions as described above.

HDAC Export Assay. Compounds are evaluated in the HDAC5 nuclear exposrt assay, a 384-well plate-based assay that enables HTS to identify small molecules that block agonist-dependent nuclear export of HDAC5. This assay employs the Cellomics High Content Imaging platform (Giuliano and Taylor, 1998) and adenovirus encoding green fluorescent protein (GFP) tagged HDAC5. Neonatal rat ventricular myocytes (NRVMs) are infected with GFP-HDAC5 encoding virus and plated on gelatin-coated 384-well dishes. Cells are exposed to compound and stimulated with a prostaglandin (PGF2α), which is a potent stimulus for HDAC5 nuclear export. Following 2 h of stimulation, cells are fixed and GFP-HDAC5 localization is quantified using the Cellomics system, which provides a readout of relative fluorescence intensity in the cytoplasmic versus nuclear compartment.

Determination of Compound Exposure. Adult male Sprague−Dawley rats, with in-dwelling jugular vein cannulae, were obtained from Harlan (Indianapolis, IN). The animals were fasted overnight prior to dosing and were fed 4 h after administration of dose. The rats were administered either a single intravenous (iv) dose (2 mg/kg, $n = 3$) or via oral (po) gavage (5 mg/kg, $n = 3$). Compound **13c** was administered as a solution in 10% NMP, 10% Cremophor EL, and 80% D5W, whereas **13y** was administered in solution formulation consisting of 10% NMP, 10% Cremophor EL, 7.8% HCl (1 N), and 70% phosphate buffer (pH 7.4), with pH adjustment made by adding 1 N NaOH. Blood samples were collected at 0.08, 0.25, 0.5, 1, 2, 4, 6, and 8 h after the iv dose and at 0.25, 0.5, 1, 2, 4, 6, and 8 h after the po dose into tubes containing EDTA. Plasma was prepared from the blood samples and analyzed for drug concentrations by LC−MS/MS.

DSS Rat Model. The 6−7 week-old male Dahl salt-sensitive (DSS) rats ($n = 50$) from Harlan Labs were fed base diet (0.49% NaCl) and allowed to acclimate for 1 week prior being separated into five weight-matched groups. Rats were maintained on the grain based diet (0.49% NaCl) or switched to grain diet containing 8.0% NaCl for 2 consecutive weeks. Coincident with diet switch rats were administered (po, 5 mL/kg) vehicle (0.5% methylcellulose, 0.5% Tween-80) or test compound **13c** or **13y** (5, 15, or 50 mg/kg) suspended in vehicle. At the completion of study, steady-state hemodynamics were determined. The rats were then sacrificed and tissues were collected for morphological and biochemical analysis.

TAB Rat Model. The 7−8 week-old male Sprague−Dawley rats ($n = 30$) from Charles River Labs were allowed normal chow and water ad libitum and allowed to acclimate for 1 week. Rats were then instrumented with an aortic occlusion cuff or underwent sham surgery. Coincident with the surgical procedure, rats were administered (sc, 1.0 mL/kg) vehicle (acidified captisol) or **13c** (15 mg/kg/day sc) solved in vehicle for two weeks. On the final day of study, end-point cardiac performance and steady-state hemodynamics were determined by ultrasound and direct cardiac catheterization, respectively. Following completion of the measurement protocol, the rats were sacrificed, and tissues were collected for morphological and biochemical analysis.

Chemistry. General. NMR spectra were recorded on a Bruker Avance II 400 MHz spectrometer. All chemical shifts are reported in parts per million (δ) relative to tetramethylsilane. The following abbreviations are used to denote signal patterns: s = singlet, d = doublet, t = triplet, m = multiplet, and br = broad. Flash chromatography was conducted using grade 60 230−400 mesh silica gel from Fisher Chemical (S825-1) or by utilizing the CombiFlash Companion from Teledyne Isco, Inc. and RediSep Rf disposable normal phase silica gel columns (4−120 g). Thin layer chromatography was performed using 2.5 cm × 7.5 cm glass-backed TLC silica gel 60 F_{254} plates from EMD Chemicals, Inc. (15341-1) and visualized by UV light. HPLC purifications were performed on a Gilson preparative HPLC system controlled by Unipoint software using X-Bridge phenyl, C8, C18, or RP18 30 mm × 50 mm columns with 5 μm particle size. The purity of all compounds was ≥95% unless otherwise noted. Low-resolution mass spectra were recorded using an Agilent 1100 series LC−MS spectrometer. *N-tert*-Butyl-2-methylnicotinamide **14d** was purchased from Astatech (catalog no. 30048).

3-Methylisonicotinonitrile (4). To 3-methylpyridine 1-oxide **3** (15.90 g, 150 mmol) was added at 0 °C during 30 min dimethyl sulfate (15.60 mL). The resulting reaction mixture was stirred overnight at 40 °C. A solution of KCN (10.75 g, 165 mmol) in a mixture of EtOH/water 1:1 (120 mL) was added, and the reaction mixture was stirred overnight at 40 °C. The reaction mixture was concentrated in vacuo, and the residue was partitioned between EtOAc and water. The aqueous phase was extracted with EtOAc, and the combined organic layers were dried over Na_2SO_4, filtered, and concentrated at reduced pressure. Purification by flash column chromatography (silica gel, cyclohexane/EtOAc 85:15) afforded the title compound as orange crystals (6.00 g, 50.80 mmol, 34%): ^{1}H NMR (400 MHz, DMSO-d_6) δ ppm 8.76 (s, 1H), 8.64 (d, $J = 4.9$ Hz, 1H), 7.80 (d, $J = 4.9$ Hz, 1H).

***N-tert*-Butyl-3-methylisonicotinamide (5).** To the solution of **4** (18.90 g, 159.92 mmol) in CH_2Cl_2 (50 mL) was added *t*-BuOAc (72.63 mL, 538.84 mmol), followed by concentrated H_2SO_4 (12.32 mL, 874.46 mmol). The mixture was stirred for 8 h at room temperature, then diluted with a solution of saturated aqueous $NaHCO_3$ and CH_2Cl_2 (50 mL). The organic layer was washed with H_2O, brine, dried over anhydrous Na_2SO_4, and then evaporated under reduced pressure to provide the title compound as a white solid (29.30 g, 152.44 mmol, 95%).

Alternatively, the title compound was prepared from isonicotinic acid **6**. Acid **6** (10 g, 80.4 mmol) was added to a 750 mL five-necked flask equipped with an overhead stirrer, internal thermometer, and nitrogen supply. Dichloromethane (300 mL) was added, and the suspension was cooled to 0 °C. Triethylamine (17.6 mL, 121 mmol) was added maintaining a temperature under 0 °C, at which time the starting material dissolved. To the clear solution, ethyl chloroformate (9.5 mL, 98.1 mmol) was added dropwise over 25 min maintaining a temperature under 0 °C. The reaction mixture was stirred at 0 °C for 30 min. *tert*-Butylamine (10.4 mL, 96.5 mmol) was added slowly to the reaction mixture at 0 °C, and the solution was allowed to warm to room temperature and stirred for 3.5 h. The reaction mixture was diluted with water (100 mL), and the dichloromethane layer was separated. The organic phase was washed with 1 M HCl (100 mL) and the aqueous phase, containing the product, neutralized to pH 9 with NaOH solution. The aqueous phase was washed twice with ethyl acetate (2 × 100 mL) and the combined organic phases were dried over Na_2SO_4, filtered, and concentrated in vacuo to give *N-tert*-butylisonicotinamide as a pale-yellow solid (9.8 g, 68.4%). MS (ESI) *m*/*z* 179 (M + 1); ^{1}H NMR (400 MHz, DMSO-d_6) δ ppm 8.66 (s, 2 H), 8.02 (br s, 1 H), 7.70 (s, 2 H), 1.37 (s, 9 H).

N-tert-butylisonicotinamide (9 g, 50.5 mmol) was added to a 750 mL five-necked flask equipped with an overhead stirrer, internal thermometer, and nitrogen supply. Tetrahydrofuran (225 mL) was added, and the clear solution was cooled to −75 °C. A solution of *n*-butyllithium 1.6 M in hexane (69 mL, 110 mmol) was added dropwise over 40 min while maintaining

the temperature under −70 °C. The reaction mixture was stirred at −70 °C for 1 h. Methyl iodide (3.5 mL, 55 mmol) was added while maintaining the temperature under −70 °C. The solution was stirred at −75 °C for 30 min and then allowed to warm to room temperature and stirred overnight. The reaction mixture was cooled to 0 °C, and a saturated aqueous solution of ammonium chloride (50 mL) was added. The reaction mixture was diluted with water (150 mL) and ethyl acetate (150 mL) and the organic layer separated. The aqueous phase was extracted with fresh ethyl acetate (150 mL). The combined organic phases were washed with brine (100 mL), dried over Na_2SO_4, filtered, and concentrated in vacuo to give a pale-yellow solid. The yellow solid was first triturated with hexane (30 mL) and then recrystallized with *tert*-butyl methyl ether (20 mL) to give **5** as a pale-yellow solid (5.1 g, 53.1%): MS (ESI) m/z 193 (M + 1); ^{1}H NMR (400 MHz, $CDCl_3$) δ ppm 8.45 (dd, J = 8.2, 4.1 Hz, 2 H), 7.17 (d, J = 8.2 Hz, 1 H), 5.60 (br s, 1 H), 2.39 (s, 3 H), 1.46 (s, 9 H).

***N*-*tert*-Butyl-3-(2-(pyridin-4-yl)-2-oxoethyl)isonicotinamide (8a).** To **5** (10.4 g, 51.4 mmol) in THF (220 mL) was added *n*-BuLi (69.0 mL, 110 mmol, 1.6 M in hexanes) at −45 °C under an inert atmosphere. The reaction mixture was stirred for 60 min at −45 °C to obtain a bright-red suspension. Then isonicotinic acid methyl ester (6.54 mL, 54.8 mmol) was added in one portion. The cooling bath was removed, and stirring was continued for 2 h at room temperature. The reaction mixture was diluted with EtOAc and washed with saturated aqueous NH_4Cl solution. The organic layer was separated, and the aqueous layer was extracted with EtOAc (3×). The combined organic layers were dried over $MgSO_4$, filtered, and evaporated to dryness. The residue was purified by column chromatography (SiO_2, gradient elution, EtOAc/MeOH 100:0 → 90:10) to yield the title compound (11.6 g, 37.1 mmol, 72%) as a pale-yellow solid: MS (ESI) m/z 298.2 (M + 1); ^{1}H NMR (400 MHz, DMSO-d_6) δ ppm 8.83 (d, 2 H), 8.56 (d, 1 H), 8.51 (s, 1 H), 8.11 (s, NH), 7.86 (d, 2 H), 7.38 (d, 1 H), 4.63 (d, 2 H), 1.21 (s, 9 H).

***N*-*tert*-Butyl-3-(2-(2-chloropyridin-4-yl)-2-oxoethyl)isonicotinamide (8b).** The title compound was prepared from **5** above and 2-chloroisonicotinic acid methyl ester by the method described above for the synthesis of **8a**: MS (ESI) m/z 332.8 (M + 1); ^{1}H NMR (400 MHz, $CDCl_3$) δ ppm 8.63 (m, 2 H), 8.48 (s, 1 H), 7.84 (s, 1 H), 7.74 (dd, J = 5.1, 1.5 Hz, 1 H), 7.33 (d, J = 5.1 Hz, 1 H), 5.90 (br s, 1 H), 4.57 (s, 2 H).

1-Bromo-3-pyridin-4-yl[2,6]naphthyridine (9a). A solution of **8a** (6.50 g, 20.8 mmol) in DMF (12 mL) was heated to 220 °C for 5 min in a microwave oven. The product, 3-pyridin-4-ylpyrano-[4,3-*c*]pyridin-1-one, precipitated from the reaction mixture and was isolated by filtration. The filtrate was heated two more times to 220 °C for 5 min in a microwave oven to give two other crops of the product. The precipitates were combined to yield 3-pyridin-4-ylpyrano[4,3-*c*]pyridin-1-one (4.05 g, 17.2 mmol, 83%) as a white solid: MS (ESI) m/z 225.1 (M + 1); ^{1}H NMR (400 MHz, DMSO-d_6) δ ppm 9.09 (s, 1H), 8.83 (d, 1H), 8.74 (d, 2H), 8.04 (d, 1H), 7.85 (m, 3H).

A suspension of 3-pyridin-4-ylpyrano[4,3-*c*]pyridin-1-one (6.70 g, 28.4 mmol) in NH_3 (7 M in MeOH) was stirred for 2 h at room temperature. The reaction mixture was evaporated to dryness to yield 3-hydroxy-3-pyridin-4-yl-3,4-dihydro-2*H*-[2,6]naphthyridin-1-one (7.12 g, 28.0 mmol, 99%) as a white solid: MS (ESI) m/z 242.3 (M + 1); ^{1}H NMR (400 MHz, DMSO-d_6) δ ppm 9.11 (s, NH), 8.65 (d, 1H), 8.60 (m, 3H), 7.79 (d, 1H), 7.58 (d, 2H), 6.72 (s, OH), 3.36 (m, 1H), 3.14 (m, 1H).

3-Hydroxy-3-pyridin-4-yl-3,4-dihydro-2*H*-[2,6]naphthyridin-1-one (1.20 g, 5.38 mmol) and $POBr_3$ (3.95 g, 13.7 mmol) were mixed under argon and heated to 130 °C for 6 h. After the mixture was cooled, ice was added and the pH adjusted to 8 with 2 N Na_2CO_3. The precipitate was filtered, washed with water, and dried to yield the title compound (1.20 g, 4.19 mmol, 78%) as brown powder: MS (ESI) m/z 287 (M + 1). The crude product was used without further purification.

1-Chloro-3-pyridin-4-yl[2,6]naphthyridine (9b). A solution of **8a** (6.50 g, 20.8 mmol) in DMF (12 mL) was heated to 220 °C for 5 min in a microwave oven. The product, 3-pyridin-4-ylpyrano-[4,3-*c*]pyridin-1-one, precipitated from the reaction mixture and was isolated by filtration. The filtrate was heated two more times to 220 °C for 5 min in a microwave oven to give two other crops of the product. The precipitates were combined to yield 3-pyridin-4-ylpyrano[4,3-*c*]pyridin-1-one (4.05 g, 17.2 mmol, 83%) as a white solid: MS (ESI) m/z 225.1 (M + 1); ^{1}H NMR (400 MHz, DMSO-d_6) δ ppm 9.09 (s, 1H), 8.83 (d, 1H), 8.74 (d, 2H), 8.04 (d, 1H), 7.85 (m, 3H).

A suspension of 3-pyridin-4-ylpyrano[4,3-*c*]pyridin-1-one (6.70 g, 28.4 mmol) in NH_3 (7 M in MeOH) was stirred for 2 h at room temperature. The reaction mixture was evaporated to dryness to yield 3-hydroxy-3-pyridin-4-yl-3,4-dihydro-2*H*-[2,6]-naphthyridin-1-one (7.12 g, 28.0 mmol, 99%) as a white solid: MS (ESI) m/z 242.3 (M + 1); ^{1}H NMR (400 MHz, DMSO-d_6) δ ppm 9.11 (s, NH), 8.65 (d, 1H), 8.60 (m, 3H), 7.79 (d, 1H), 7.58 (d, 2H), 6.72 (s, OH), 3.36 (m, 1H), 3.14 (m, 1H).

A suspension of 3-hydroxy-3-pyridin-4-yl-3,4-dihydro-2*H*-[2,6]-naphthyridin-1-one (3.00 g, 11.8 mmol) in $POCl_3$ (50 mL) was heated to 80 °C for 24 h. The reaction mixture was concentrated under reduced pressure to remove excess $POCl_3$. The residual oil was treated with ice-cold H_2O, and the suspension thus obtained was basified to pH 14 with 10 N NaOH while keeping the temperature below room temperature. The mixture was filtered and the aqueous filtrate was extracted with CH_2Cl_2 (2×). The combined organic layers were dried over $MgSO_4$, filtered, and evaporated to dryness to yield a first crop of the crude title compound. The gluey precipitate obtained from the filtration was extracted with CH_2Cl_2 (stirring for 10 min at room temperature, 2×) to yield a second crop of the crude title compound. The combined crude products were purified by column chromatography (SiO_2, gradient elution, CH_2Cl_2/MeOH 100:0 → 94:6) to yield the title compound (932 mg, 3.78 mmol, 32%) as a white solid: MS (ESI) m/z 242.2 (M + 1); ^{1}H NMR (400 MHz, DMSO-d_6) δ ppm 9.56 (s, 1H), 8.89 (m, 2H), 8.76 (m, 2H), 8.11 (m, 3H).

1-Chloro-3-(2-chloropyridin-4-yl)-2,6-naphthyridine (9c). Compound **8b** above (6.83 g, 20.46 mmol) was suspended in acetic acid and heated at 100 °C overnight. The mixture was cooled to room temperature and evaporated under reduced pressure. To the residue was added H_2O, and the product was extracted with EtOAc. The combined organic layers were washed with brine, dried over anhydrous Na_2SO_4, and then concentrated. The solid was triturated with Et_2O to give 3-(2-chloropyridin-4-yl)-1*H*-pyrano[4,3-*c*]pyridin-1-one as an off-white solid (60%): MS (ESI) m/z 259.7 (M + 1); ^{1}H NMR (400 MHz, $CDCl_3$) δ ppm 9.12 (s, 1 H), 8.86 (d, J = 5.5 Hz, 1 H), 8.56 (d, J = 5.5 Hz, 1 H), 8.18 (d, J = 5.1 Hz, 1 H), 8.03 (s, 1 H), 7.93 (d, J = 5.1 Hz, 1 H), 7.77 (s, 1 H).

3-(2-Chloropyridin-4-yl)-1*H*-pyrano[4,3-*c*]pyridin-1-one (1.66 g, 6.41 mmol) was suspended in EtOH (35 mL). To the suspension was added 28.5% NH_4OH (26 mL) at room temperature, and the mixture was stirred overnight. The solvent was then evaporated, and the residue was dried under reduced pressure at 45 °C for 30 min to provide a white solid. The crude product was suspended in EtOH (35 mL), treated with 4 N HCl (8.7 mL), and stirred overnight at room temperature. The mixture was filtered, and the solid obtained was dried under high vacuum (1.50 g, 91%): MS (ESI) m/z 257.7 (M + 1); ^{1}H NMR (400 MHz, $CDCl_3$) δ ppm 9.51 (s, 1 H), 8.84 (d, J = 6.1 Hz, 1 H), 8.72 (d, J = 6.1 Hz, 1 H), 8.62 (d, J = 5.0 Hz, 1 H), 7.95 (s, 1 H), 7.80 (d, J = 5.0 Hz, 1 H), 7.38 (s, 1 H).

A mixture of 3-(2-chloropyridin-4-yl)-2,6-naphthyridin-1-ol (1.29 g, 5.02 mmol), $POCl_3$ (35 mL), and tetramethylammonium chloride (2.6 g, 23.72 mmol) was refluxed at 110 °C for 36 h. The $POCl_3$ was removed by distillation, and ice cold 10% K_2CO_3 was added carefully. The mixture was extracted with EtOAc, washed with water and then brine, dried over anhydrous

Na_2SO_4, and concentrated under reduced pressure. The crude residue was washed with cold methanol (5 mL) to give the title compound as a greenish brown solid (1.05 g, 3.80 mmol, 76%): MS (ESI) m/z 277.1 (M + 1); ^{1}H NMR (400 MHz, $CDCl_3$) δ ppm 9.55 (s, 1 H), 8.88 (d, J = 6.1 Hz, 1 H), 8.75 (s, 1 H), 8.55 (d, J = 5.6 Hz, 1 H), 8.27 (s, 1 H), 8.25 (d, J = 6.1 Hz, 1 H), 8.18 (d, J = 5.5 Hz, 1 H).

3-(2-Chloropyridin-4-yl)-1-methoxy[2,6]naphthyridine (23). To a solution of **9c** (0.91 g, 3.3 mmol) in methanol (20 mL) was added sodium methoxide (0.27 g, 5 mmol). The mixture was refluxed for 3 h and cooled to room temperature. Volatiles were removed by rotary evaporation, and the residue was partitioned between water and CH_2Cl_2. The separated aqueous phase was extracted twice with CH_2Cl_2, and the combined organics were washed with water and brine, dried (Na_2SO_4), filtered, and concentrated in vacuo. The residue was chromatographed on silica gel to give a light-yellow solid (0.80 g, 89%): MS (ESI) m/z 272.1 (M + 1); ^{1}H NMR (400 MHz, $CDCl_3$) δ ppm 9.3 (s, 1 H), 8.75 (d, J = 6.3 Hz, 1 H), 8.5 (s, 1 H), 8.08 (s, 1 H), 8.02 (d, J = 5.6 Hz, 1 H), 7.93 (dd, J = 5.1, 1.4 Hz, 1 H), 7.86 (s, 1 H), 4.28 (s, 3 H).

[4-(1-Chloro[2,6]naphthyridin-3-yl)pyridin-2-yl]cyclohexylamine (24). To a solution of methoxynaphthyridine **23** (0.43 g, 1.29 mmol) in wet *tert*-butyl alcohol (10 mL) is added potassium *tert*-butoxide (1 M in THF, 6.4 mL, 6.4 mmol), and the mixture was heated at 100 °C overnight. After the volatiles were removed under reduced pressure, the residue was suspended in water. The pH was adjusted to 7, and the resulting solid was filtered and air-dried. The crude solid (406 mg, 94%) was pure by LCMS and used directly in the next step without further purification: MS (ESI) m/z 321.3 (M + 1).

A mixture of the naphthyridinone above (360 mg, 1.1 mmol) and tetramethylammonium chloride (100 mg) in $POCl_3$ (15 mL) was heated at 110 °C overnight. Volatiles were removed by evaporation, and the residue was treated with ice, basified with 1 N NaOH, and extracted with CH_2Cl_2 (3 × 20 mL). The combined organic layers were dried over Na_2SO_4, filtered, and concentrated. The residue was chromatographed on silica gel to give the product (260 mg, 68%): MS (ESI) m/z 339.2 (M + 1); ^{1}H NMR (400 MHz, $CDCl_3$) δ ppm 9.26 (s, 1 H), 8.61 (d, J = 5.4 Hz, 1 H), 8.18 (d, J = 5.2 Hz, 1 H), 7.79 (d, J = 6.0 Hz, 1 H), 7.75 (s, 1 H), 7.21 (s, 1 H), 7.20 (d, J = 5.4 Hz, 1 H), 4.64 (d, J = 8.0 Hz, 1 H), 3.69 (br 1 H), 2.12 (m, 2 H), 1.79 (m, 2 H), 1.67 (m, 1 H), 1.6−1.4 (m, 5 H).

[2-(3-Pyridin-4-yl[2,6]naphthyridin-1-ylamino)ethyl]carbamic Acid *tert*-Butyl Ester (10a). Bromide **9a** (200 mg, 0.70 mmol) and (2-aminoethyl)carbamic acid *tert*-butyl ester (172 mg, 1.05 mmol) in dioxane (30 mL) was heated with 5 drops of 40% NaOH to 110 °C for 3 days. After cooling, the reaction mixture was diluted with water and extracted with ethyl acetate. The combined organic layers were dried over sodium sulfate, filtered, and concentrated. The residue was purified by chromatography (ethyl acetate/ethanol 9:12), yielding the title compound (110 mg, 0.30 mmol, 42%) as a light-brown powder: MS (ESI) m/z 366.2 (M + 1); ^{1}H NMR (400 MHz, DMSO-d_6) δ ppm 9.23 (s, 1 H), 8.69 (d, J = 6.0 Hz, 2 H), 8.63 (d, J = 6.6 Hz, 1 H), 8.18 (d, J = 6.0 Hz, 2 H), 8.12 (d, J = 6.6 Hz, 1 H), 7.96 (md, 1 H), 7.88 (s, 1 H), 7.05 (m, 1 H), 3.68 (m, 2 H), 3.33 (m, 2 H), 1.39 (s, 9 H).

3-(3-Pyridin-4-yl[2,6]naphthyridin-1-ylamino)propan-1-ol (10b). Bromide **9a** (250 mg, 0.87 mmol) and 1-hydroxypropylamine (657 mg, 8.74 mmol) in THF (10 mL) were heated to 45 °C for 2 h. After cooling, the reaction mixture was concentrated under reduced pressure and the residue purified by chromatography (ethyl acetate/ethanol 8:2), yielding the title compound (50 mg, 0.18 mmol, 20%) as a yellow powder: MS (ESI) m/z 281.3 (M + 1); ^{1}H NMR (400 MHz, DMSO-d_6) δ ppm 9.24 (s, 1 H), 8.73 (d, J = 6.0 Hz, 2 H), 8.64 (d, J = 6.6 Hz, 1 H), 8.17 (d, J = 6.6 Hz, 1 H), 8.15 (d, J = 6.0 Hz, 2 H), 7.91 (m, 1 H), 7.87 (s, 1 H), 4.54 (m, 1 H), 3.70 (m, 2 H), 3.58 (m, 2 H), 1.92 (m, 2 H).

***N**1*-(3-Pyridin-4-yl[2,6]naphthyridin-1-yl)ethane-1,2-diamine (2).** Compound **10a** (80 mg, 0.22 mmol) was stirred in TFA (0.7 mL) and CH_2Cl_2 (20 mL) for 10 min at 0 °C and at room temperature for 4 h. The reaction mixture was concentrated. Twice CH_2Cl_2 was added and the mixture concentrated. The residue was crystallized from diethyl ether to yield the title compound (94 mg, 0.17 mmol, 78%) as yellow crystals (TFA salt): MS (ESI) m/z 266.1 (M + 1); ^{1}H NMR (400 MHz, DMSO-d_6) δ ppm 9.32 (s, 1 H), 8.88 (d, J = 6.0 Hz, 2 H), 8.74 (d, J = 6.6 Hz, 1 H), 8.49 (d, J = 6.0 Hz, 2 H), 8.17 (m, 3 H), 7.94 (m, 2 H), 3.91 (m, 2 H), 3.25 (m, 2 H).

1-Piperazin-1-yl-3-pyridin-4-yl[2,6]naphthyridine (11). To a solution of chloride **9b** (50 mg, 0.197 mmol) in DMF (0.5 mL) was added piperazine-1-carboxylic acid *tert*-butyl ester (77 mg, 0.393 mmol) and K_2CO_3 (55 mg, 0.393 mmol) at room temperature. The reaction mixture was heated to 90 °C and stirred for 5 h. The reaction mixture was cooled to room temperature, diluted with EtOAc, and washed with H_2O (1×). The organic layer was separated, and the aqueous layer was extracted with EtOAc (3×). The combined organic layers were dried over $MgSO_4$, filtered, and evaporated to dryness. The residue was purified by silica gel chromatography (4 g of SiO_2, gradient hexane/EtOAc 80:20 → 0:100) to afford 4-(3-pyridin-4-yl[2,6]naphthyridin-1-yl)piperazine-1-carboxylic acid *tert*-butyl ester (**10c**) as a pale-yellow solid. Compound **10c** was dissolved in TFA (0.5 mL) and CH_2Cl_2 (0.5 mL) and was stirred for 1 h at room temperature. The reaction mixture was concentrated under reduced pressure. The residue was purified by preparative reverse phase HPLC (Waters) to yield the title compound as a yellow solid (25 mg, 0.048 mmol, 25% over two steps, 2TFA salt): MS (ESI) m/z 292.3 (M + 1); ^{1}H NMR (600 MHz, DMSO-d_6) δ ppm 9.46 (s, 1 H), 9.06 (br s, 2 H), 8.88 (d, J = 6.3 Hz, 2 H), 8.74 (d, J = 5.7 Hz, 1 H), 8.57 (s, 1 H), 8.42 (d, J = 6.1 Hz, 2 H), 8.06 (d, J = 5.9 Hz, 1 H), 3.75 (br s, 4 H), 3.43 (br s, 4 H).

4-[3-(2-Chloropyridin-4-yl)[2,6]naphthyridin-1-yl]piperazine-1-carboxylic Acid *tert*-Butyl Ester (12b). To a suspension of **9c** (2.00 g, 7.20 mmol) in anhydrous ethanol (24 mL) in a dried pressure vessel was added triethylamine (3.20 mL, 23 mmol) followed by piperazine-1-carboxylic acid *tert*-butyl ester (1.70 g, 9.10 mmol). The vessel was flushed with nitrogen and then sealed. The suspension was heated in a 100 °C oil bath for 20 h. The dark-brown, nearly homogeneous reaction mixture was cooled to room temperature, then concentrated in vacuo. The residue was diluted with dichloromethane and water. The layers were agitated and separated, and the aqueous layer was extracted twice with CH_2Cl_2. The combined organic layers were dried over sodium sulfate, filtered, and concentrated. The material was purified by silica gel chromatography (120 g SiO_2, gradient 0% → 2.5% methanol/dichloromethane) to afford a brownish yellow solid, which was refluxed in 60 mL of diethyl ether. The mixture was cooled to room temperature and filtered to provide the title compound as a white solid (2.2 g, 71%): MS (ESI) m/z 426.2 (M + 1); ^{1}H NMR (400 MHz, DMSO-d_6) δ ppm 9.39 (d, J = 0.8 Hz, 1 H), 8.70 (d, J = 5.8 Hz, 1 H), 8.55 (dd, J = 5.3, 0.5 Hz, 1 H), 8.24 (dd, J = 1.5, 0.8 Hz, 1 H), 8.18 (dd, J = 5.3, 1.5 Hz, 1 H), 7.96 (d, J = 5.8 Hz, 1 H), 3.64 (br m, 4 H), 3.52 (m, 4 H), 1.45 (s, 9 H).

3-(2-Chloropyridin-4-yl)-1-piperazin-1-yl[2,6]naphthyridine (12c). A solution of compound **9c** above (700 mg, 2.53 mmol) and piperazine (262 mg, 3.04 mmol) in NMP (12 mL) was heated to 70 °C overnight. After the mixture was cooled, a yellow solid was collected by filtration and washed with MeOH (5 mL) to afford the title compound: MS (ESI) m/z 326.2, 328.2 (M + 1); ^{1}H NMR (400 MHz, MeOD) δ ppm 10.00 (s, 1 H), 9.28 (d, J = 5.6 Hz, 1 H), 9.07 (d, J = 5.1 Hz, 1 H), 8.79 (m, 4 H), 4.43 (m, 4 H), 4.11 (m, 4 H).

3-(2-Chloropyridin-4-yl)-1-(4-cyclopropylmethylpiperazin-1-yl)-[2,6]naphthyridine (12d). The title compound was prepared from **9c** (200 mg, 0.72 mmol) and *N*-cyclopropylmethylpiperazine (140 μL, 0.94 mmol) by heating in Et_3N (6 μL, 4.3 mmol) and EtOH (5 mL) in a sealed tube at 100 °C overnight. The volatiles were removed in vacuo and the residue was purified by flash chromatography, eluting with 0−10% MeOH/CH_2Cl_2 to afford

the title compound in 68% yield as a yellow solid: MS (ESI) m/z 380.3 (M + 1).

3-(2-Chloropyridin-4-yl)-1-(4-cyclopropylpiperazin-1-yl)[2,6]-naphthyridine (12e). The title compound was prepared from **9c** and *N*-cyclopropylpiperazine by analogy to the method outlined in example **12b**: MS (ESI) m/z 366.3 (M + 1).

1-{4-[3-(2-Chloropyridin-4-yl)[2,6]naphthyridin-1-yl]piperazin-1-yl}ethanone (12f). The title compound was prepared from **9c** and *N*-acetylpiperazine by analogy to the method outlined in example **12b**: MS (ESI) m/z 368.1 (M + 1).

2-[3-(2-Chloropyridin-4-yl)[2,6]naphthyridin-1-ylamino]ethanol (12g). A solution of compound **9c** (536 mg, 1.94 mmol) and 2-aminoethanol (1.50 mL, 25.2 mmol) in NMP (15 mL) was heated to 100 °C overnight. After the mixture was cooled, the volatiles were removed in vacuo and the residue was purified by RP-HPLC (3−50% CH_3CN in H_2O) to afford the title compound as a yellow solid: MS (ESI) m/z 301.1 (M + 1); ^{1}H NMR (600 MHz, DMSO-d_6) δ ppm 9.55 (m, 1 H), 8.83 (m, 1 H), 8.71 (m, 1 H), 8.57 (d, J = 5.3 Hz, 1 H), 8.17 (m, 1 H), 8.12 (dd,, J = 5.3, 1.4 Hz, 1 H), 8.10 (s, 1 H), 3.75−3.76 (m, 4 H).

4-[3-(2-Chloropyridin-4-yl)[2,6]naphthyridin-1-yl]piperazin-2-one (12h). The title compound was prepared from **9c** and piperazin-2-one by analogy to the method outlined in example **12b**: MS (ESI) m/z 340.1 (M + 1); ^{1}H NMR (400 MHz, DMSO-d_6) δ ppm 9.78 (s, 1 H), 9.10 (d, J = 5.6 Hz, 1 H), 8.96 (d, J = 5.1 Hz, 1 H), 8.85 (s, 1 H), 8.64 (s, 1 H), 8.59 (m, 1 H), 8.59 (m, 1 H), 8.41 (m, 2 H), 4.54 (m, 2 H), 4.22 (m, 2 H), 3.83 (m, 2 H).

{1-[3-(2-Chloropyridin-4-yl)[2,6]naphthyridin-1-yl]piperidin-4-ylmethyl}carbamic Acid *tert*-Butyl Ester (12i). The title compound was prepared from **9c** and piperidin-4-ylmethylcarbamic acid *tert*-butyl ester by analogy to the method outlined in **12b**: MS (ESI) m/z 454.3 (M + 1).

1-[3-(2-Chloropyridin-4-yl)[2,6]naphthyridin-1-yl]piperidine-4-carboxylic Acid Amide (12j). To a suspension of **9c** (200 mg, 0.72 mmol) in anhydrous ethanol (2.4 mL) in a sealable vial was added triethylamine (0.32 mL, 2.3 mmol) followed by isonipecotamide (120 mg, 0.90 mmol). The vial was flushed with nitrogen and then sealed. The mixture was heated in a 100 °C oil bath for 16 h. The heterogeneous mixture was cooled to room temperature, then filtered. The filtrate was washed with ethanol and dried under high vacuum to give the title compound as a yellowish brown solid (230 mg, 87%): MS (ESI) m/z 368.1 (M + 1); ^{1}H NMR (400 MHz, DMSO-d_6) δ ppm 9.36 (s, 1 H), 8.68 (d, J = 5.8 Hz, 1 H), 8.55 (d, J = 5.8 Hz, 1 H), 8.38 (s, 1H), 8.23 (s, 1 H), 8.18 (dd, J = 5.3, 1.5 Hz, 1 H), 7.89 (d, J = 5.8 Hz, 1 H), 7.34 (br s, 1 H), 6.82 (br s, 1 H), 4.05 (d, J = 12.6 Hz, 2 H), 3.09 (m, 2 H), 2.43 (m, 1 H), 1.91 (br m, 4 H).

1-[3-(2-Chloropyridin-4-yl)[2,6]naphthyridin-1-yl]piperidine-4-carboxylic Acid Methylamide. (12k). The title compound was prepared from **9c** and *N*-methylisonipecotamide by analogy to the method outlined in example **12b**: MS (ESI) m/z 382.1 (M + 1).

1-[3-(2-Chloropyridin-4-yl)[2,6]naphthyridin-1-yl]piperidine-4-carboxylic Acid Methyl Ester (12l). A solution of **9c** (1.0 g, 3.62 mmol), Et_3N (1.50 mL, 10.9 mmol), methyl isonipecotate (0.74 mL, 5.43 mmol), and DMSO (4 mL) was heated to 80 °C for 3 h. At that time, the solution was allowed to cool to room temperature and was slurried with 15 mL of water. The mixture was then poured into 200 mL of ice water. After 10 min the solid was collected via filtration. The solid was then dried under vacuum to give (1.25 g) the title compound as a brown solid: MS (ESI) m/z 383.1 (M + 1); ^{1}H NMR (400 MHz, $CDCl_3$) δ ppm 9.29 (s, 1 H), 8.67 (d, J = 5.8 Hz, 1 H), 8.49 (d, J = 4.8 Hz, 1 H), 8.07 (s, 1 H), 7.95 - 7.91 (m, 1 H), 7.83 (s, 1 H), 7.79 (d, J = 5.8 Hz, 1 H), 4.07 - 3.96 (m, 2 H), 3.76 (s, 3 H), 3.27−3.14 (m, 2 H), 2.73−2.61 (m, 1 H), 2.23−2.01 (m, 4 H).

1-(3-Hydroxypropylamino-3-(2-methylaminopyridin-4-yl)[2,6]-naphthyridine (13a). Compound **12a** (120 mg, 0.36 mmol) and methylamine (5 mL, 33% in ethanol) were heated in an autoclave at 135 °C for 4 d. The reaction mixture was cooled, concentrated, and purified by chromatography (ethyl acetate/ethanol 8:2) to give the title compound (90 mg, 0.29 mmol, 82%) as a yellow powder: MS (ESI) m/z 310.4 (M + 1); ^{1}H NMR (400 MHz, DMSO-d_6) δ ppm 9.22 (s, 1 H), 8.59 (d, J = 6.6 Hz, 1 H), 8.14 (d, J = 6.6 Hz, 1 H), 8.08 (d, J = 6.0 Hz, 1 H), 7.82 (t, J = 4.5 Hz, 1 H), 7.64 (s, 1 H), 7.27 (s, 1 H), 7.21 (d, J = 6.0 Hz, 1 H), 6.60 (d, J = 3.0 Hz, 1 H), 4.53 (t, J = 5.2 Hz, 1 H), 3.69 (m, 2 H), 3.59 (m, 2 H), 2.85 (d, J = 3.6 Hz, 3 H), 1.90 (m, 2 H).

4-[3-(2-Cyclohexylaminopyridin-4-yl)[2,6]naphthyridin-1-yl]-piperazine-1-carboxylic Acid *tert*-Butyl Ester (13b). Compound **12b** (2.30 g, 5.4 mmol), cyclohexylamine (1.24 mL, 10.8 mmol), NaO-*t*-Bu (1.04 g, 10.8 mmol), and Pd(P-*t*-Bu_3)$_2$ in dioxane (54 mL) were heated under an Ar atmosphere in a sealed tube at 130 °C overnight. After cooling, the mixture was concentrated under reduced pressure. The residue was diluted with 20% acetone/CH_2Cl_2 and filtered through Celite. The filter cake was washed successively with EtOH, acetone, CH_3CN, and MeOH. The combined filtrate was concentrated under reduced pressure. The residue was diluted with EtOAc (400 mL) and washed with water (3 × 100 mL). The separated EtOAc layer was dried (Na_2SO_4), filtered, and concentrated under reduced pressure. The residue was purified by column chromatography using 20% acetone/CH_2Cl_2 to afford the title compound: MS (ESI) m/z 489.2 (M + 1).

Cyclohexyl-[4-(1-piperazin-1-yl[2,6]naphthyridin-3-yl)pyridin-2-yl]amine (13c). To a solution of **13b** (1.34 g, 2.74 mmol) in CH_2Cl_2 (33 mL) was added TFA (6.6 mL). After 1 h and complete removal of the BOC group as judged by TLC, the mixture was diluted with CH_2Cl_2 (200 mL) and a 1 M soluton of NaOH (100 mL). The separated organic phase was washed with fresh 1 M NaOH. The combined aqueous phases were extracted with fresh CH_2Cl_2 (2 × 100 mL). The combined organic phasese were dried (Na_2SO_4), filtered, and concentrated under reduced pressure to afford the title compound: MS (ESI) m/z 389.3 (M + 1); ^{1}H NMR (400 MHz, CD_3OD) δ ppm 9.35 (s, 1 H), 8.62 (d, J = 6.1 Hz, 1 H), 8.07 (s, 1 H), 8.05 (d, J = 5.5 Hz, 1 H), 8.02 (d, J = 5.6 Hz, 1 H), 7.44 (s, 1 H), 7.30 (d, J = 5.6 Hz, 1 H), 3.80−3.71 (m, 1 H), 3.71 (s, 1 H), 3.63 (t, J = 4.8 Hz, 4 H), 3.20 (t, J = 4.8 Hz, 4 H), 2.15-2.08 (m, 2 H), 1.90−1.82 (m, 2 H), 1.78−1.71 (m, 1 H), 1.58−1.46 (m, 2 H), 1.40−1.09 (m, 3 H).

Cyclohexyl-{4-[1-(4-isobutylpiperazin-1-yl)[2,6]naphthyridin-3-yl]pyridin-2-yl}amine (13d). To a solution of **13c** (260 mg, 0.62 mmol) and 2-methylpropionaldehyde (54 mg, 0.76 mmol) in CH_2Cl_2 (5 mL) was added $NaBH(OAc)_3$ (540 mg, 2.7 mmol). The suspension was stirred at room temperature for 24 h. A saturated aqueous solution of $NaHCO_3$ (5 mL) was added, and the mixture was extracted with CH_2Cl_2 (3 × 10 mL). The combined organic layers were dried (Na_2SO_4), filtered, and concentrated under reduced pressure. The oily residue was purified by RP-HPLC (30−90% CH_3CN in H_2O to afford the title compound as a white solid: HRMS (ESI) m/z 445.3087 (M + 1); ^{1}H NMR (400 MHz, $CDCl_3$) δ ppm 9.26 (s, 1 H), 8.61 (d, J = 5.7 Hz, 1 H), 8.20−8.14 (m, 1 H), 7.81 (d, J = 5.8 Hz, 1 H), 7.75 (s, 1 H), 7.24−7.18 (m, 2 H), 4.61 (d, J = 7.7 Hz, 1 H), 3.77−3.65 (m, 1 H), 3.65−3.57 (m, 4 H), 2.74−2.65 (m, 3 H), 2.22 (d, J = 7.3 Hz, 2 H), 2.13 (dd, J = 12.6, 3.2 Hz, 2 H), 1.98−1.74 (m, 4 H), 1.73−1.62 (m, 1 H), 1.54−1.38 (m, 2 H), 1.35−1.20 (m, 3 H), 0.96 (d, J = 6.6 Hz, 6 H).

4-{3-[2-(Tetrahydropyran-4-ylamino)pyridin-4-yl][2,6]naphthyridin-1-yl}piperazine-1-carboxylic Acid *tert*-Butyl Ester (13e). To a dried sealable vial was added **12b** (180 mg, 0.43 mmol), sodium *tert*-butoxide (120 mg, 1.30 mmol), and dioxane (6.1 mL). The dark-red solution was sparged with argon for 10 min. 4-Aminotetrahydropyran (0.16 mL, 1.30 mmol) was added via syringe, followed by palladium(0)tris(tri-*tert*-butylphosphine) (44 mg, 0.09 mmol). The vial was flushed with argon, then sealed and heated in a 120 °C oil bath for 14 h. The dark-brown solution was cooled to room temperature, then diluted with water and CH_2Cl_2. The layers were agitated and separated. The aqueous layer was extracted twice with CH_2Cl_2. The combined organic layers were dried over sodium sulfate, filtered, and concentrated to give a

brown residue. Purification via silica gel chromatography (40 g of SiO_2, gradient 70% → 100% ethyl acetate/hexanes followed by 0% → 10% MeOH/CH_2Cl_2) afforded the title compound as a brown solid (120 mg, 80% pure) as judged by ^{1}H NMR: MS (ESI) m/z 491.5 (M + 1).

4-(1-Piperazin-1-yl[2,6]naphthyridin-3-yl)pyridin-2-yl](tetrahydropyran-4-yl)amine (13f). To a suspension of **13e** (120 mg, 0.25 mmol) in 1.80 mL of CH_2Cl_2 at 0 °C is added 0.60 mL of TFA drop by drop via pipet. The resulting brownish orange solution is warmed to room temperature and stirred for 1 h and then concentrated in vacuo to afford an amber oil. The residue was dissolved in MeOH and a small amount of water, then purified via preparative reverse-phase HPLC (X-Bridge C_{18} column, flow rate = 40 mL/min, gradient 10% → 80% acetonitrile/5 mM aqueous ammonium hydroxide over 20 min) to give the title compound as a pale-yellow solid (66 mg, 68%): MS (ESI) m/z 391.2 (M + 1); ^{1}H NMR (400 MHz, CD_3OD) δ ppm 9.30 (d, J = 1.0 Hz, 1 H), 8.58 (d, J = 5.8 Hz, 1 H), 8.03 (m, 2 H), 7.98 (d, J = 5.8 Hz, 1 H), 7.42 (s, 1H), 7.29 (dd, J = 5.7, 1.6 Hz, 1 H), 3.99 (m, 3 H), 3.59 (m, 6H), 3.14 (dd, J = 5.6, 4.0 Hz, 4 H), 2.03 (dd, J = 12.2, 2.8 Hz, 2 H), 1.58 (m, 2 H).

{4-[1-(4-Isobutylpiperazin-1-yl)[2,6]naphthyridin-3-yl]pyridin-2-yl}(tetrahydropyran-4-yl)amine (13g). The title compound is prepared by reductive amination of **13f** commercially with available 2-methylpropionaldehyde. Thus, sodium triacetoxyborohydride (339 mg, 1.59 mmol) is added to a solution of **13f** (148 mg, 0.38 mmol) and 2-methylpropionaldehyde (42 μL, 0.46 mmol) in methylene chloride (8 mL) and stirred for 12 h. The mixture is concentrated on a rotary evaporator and partially purified on a 12 g (Redisep, Isco) silica gel column with a 0−10% methanol/methylene chloride gradient. The resulting product is further purified by reverse phase HPLC using a 30−95% acetonitrile/water gradient. This yields 41.2 mg (24%) after consolidation and concentration of fractions: HRMS (ESI) m/z 447.2717 (M + 1); ^{1}H NMR (400 MHz, $CDCl_3$) δ ppm 9.29 (s, 1 H), 8.64 (d, J = 5.8 Hz, 1 H), 8.22 (d, J = 5.3 Hz, 1 H), 7.84 (d, J = 5.8 Hz, 1 H), 7.78 (s, 1 H), 7.30−7.28 (m, 1 H), 7.27 (s, 1 H), 4.57 (d, J = 8.0 Hz, 1 H), 4.15−3.98 (m, 3 H), 3.73−3.53 (m, 6 H), 2.73 (t, J = 4.6 Hz, 4 H), 2.25 (d, J = 7.3 Hz, 2 H), 2.15 (dd, J = 12.6, 2.1 Hz, 2 H), 1.98−1.77 (m, 1 H), 1.70−1.54 (m, 2 H), 0.99 (d, J = 6.6 Hz, 6 H).

Cyclohexyl-{4-[1-((*cis*-3,5-dimethylpiperazin-1-yl)[2,6]naphthyridin-3-yl]pyridin-2-yl}amine (13h). The title compound was prepared from chloride **24** and *cis*-3,5-dimethylpiperazine by analogy to the preparation of **13i** below: MS (ESI) m/z 417.4 (M + 1); ^{1}H NMR (400 MHz, $CDCl_3$) δ ppm 9.3 (s, 1 H), 8.6 (d, 1 H), 8.2 (d, 1 H), 7.8 (d, 1 H), 7.7 (s, 1 H), 7.2 (m, 2 H), 4.7 (br s, 1 H), 3.9 (d, 2 H), 3.7 (br s, 5 H), 3.3 (br s, 2 H), 2.7 (t, 2 H), 2.1 (m, 2 H), 1.5 (m, 8 H), 1.2 (d, 6 H).

Cyclohexyl-{4-[1-(4-methylpiperazin-1-yl)[2,6]naphthyridin-3-yl]pyridin-2-yl}amine (13i). A solution of chloronaphthyridine **24** (34 mg, 0.1 mmol) and 1-methylpiperazine (0.033 mL, 0.3 mmol) in 2-methoxyethanol (4 mL) was heated by microwave at 200 °C for 30 min. The mixture was then poured onto a solid phase extraction (SPE) cartridge containing strong cation exchanger (SCX) as the media (2 g). After the sample was washed with MeOH (10 mL), the product was eluted with 20:2:1 EtOAc−MeOH−Et_3N. The eluent was concentrated in vacuo and the residue was chromatographed on silica gel to give the product (40 mg, 99%): MS (ESI) m/z 403.4 (M + 1); ^{1}H NMR (400 MHz, $CDCl_3$) δ ppm 9.3 (s, 1 H), 8.6 (d, 1 H), 8.2 (d, 1 H), 7.8 (m, 2 H), 7.2 (m, 2 H), 4.8 (br s, 1 H), 3.6 (br s, 5 H), 2.8 (br s, 4 H), 2.4 (s, 3 H), 2.1 (m, 2 H), 1.8 (m, 2 H), 1.7 (m, 1 H), 1.5 (m, 2 H), 1.3 (m, 3 H).

1-[3-(2-Cyclohexylaminopyridin-4-yl)[2,6]naphthyridin-1-yl]-piperidin-4-ol (13j). The title compound was prepared from chloride **24** and 4-hydroxypiperidine by analogy to the preparation of **13i** above: MS (ESI) m/z 404.4 (M + 1); ^{1}H NMR (400 MHz, $CDCl_3$) δ ppm 9.3 (s, 1 H), 8.6 (d, 1 H), 8.1 (d, 1 H), 7.8 (m, 2 H), 7.2 (m, 2 H), 5.6 (br s, 1 H), 4.0 (m, 1 H), 3.9 (m, 2 H), 3.6 (m, 1 H), 3.4 (m, 2 H), 2.1−1.2 (m, 14 H).

Cyclohexyl-{4-[1-(4-cyclopropylmethylpiperazin-1-yl)[2,6]naphthyridin-3-yl]pyridin-2-yl}amine (13k). The title compound was prepared from **12d** and cyclohexylamine by analogy to the method described for the preparation of **13e** above: HRMS (ESI) m/z 443.2924 (M + 1); ^{1}H NMR (400 MHz, $CDCl_3$) δ ppm 9.27 (s, 1 H), 8.61 (d, J = 5.8 Hz, 1 H), 8.18 (d, J = 5.3 Hz, 1 H), 7.80 (d, J = 5.8 Hz, 1 H), 7.76 (s, 1 H), 7.25−7.16 (m, 2 H), 4.59 (d, J = 8.1 Hz, 1 H), 3.79−3.57 (m, 5 H), 2.84 (t, J = 4.6 Hz, 4 H), 2.40 (d, J = 6.6 Hz, 2 H), 2.19−2.06 (m, 2 H), 1.88−1.73 (m, 2 H), 1.73−1.61 (m, 1 H), 1.55−1.37 (m, 2 H), 1.36−1.19 (m, 3 H), 1.03−0.87 (m, 1 H), 0.64−0.51 (m, 2 H), 0.18 (q, J = 4.9 Hz, 2 H).

Cyclohexyl-{4-[1-(4-cyclopropylpiperazin-1-yl)[2,6]naphthyridin-3-yl]pyridin-2-yl}amine (13l). The title compound was prepared from **12e** and cyclohexylamine by analogy to the method described for the preparation of **13e** above: HRMS (ESI) m/z 429.2768 (M + 1); ^{1}H NMR (400 MHz, $CDCl_3$) δ ppm 9.27 (s, 1 H), 8.62 (d, J = 5.8 Hz, 1 H), 8.18 (d, J = 5.4 Hz, 1 H), 7.81 (d, J = 5.8 Hz, 1 H), 7.76 (s, 1 H), 7.24−7.17 (m, 2 H), 4.60 (d, J = 7.9 Hz, 1 H), 3.76−3.63 (m, 1 H), 3.63−3.52 (m, 3 H), 2.98−2.85 (m, 4 H), 2.19−2.07 (m, 2 H), 1.90−1.73 (m, 4 H), 1.70 (d, J = 3.4 Hz, 1 H), 1.55−1.38 (m, 2 H), 1.35−1.19 (m, 3 H), 0.60−0.46 (m, 4 H).

1-{4-[3-(2-Cyclohexylaminopyridin-4-yl)[2,6]naphthyridin-1-yl]-piperazin-1-yl}ethanone (13m). The title compound was prepared from **12f** and cyclohexylamine by analogy to the method described for the preparation of **13e** above: MS (ESI) m/z 431.4 (M + 1); ^{1}H NMR (400 MHz, CD_3OD) δ ppm 9.31 (d, 1 H), 8.60 (d, 1 H), 8.04 (s, 1 H), 8.00 (m, 2 H), 7.37 (d, 1 H), 7.22 (d, 1 H), 3.88 (br d, 4 H), 3.70 (m, 1 H), 3.61 (br d, 4 H), 2.19 (s, 3 H), 2.08 (br m, 2 H), 1.80 (m, 2 H), 1.69 (br d, 1 H), 1.47 (m, 2 H), 1.28 (m, 3 H).

2-[3-(2-Cyclohexylaminopyridin-4-yl)[2,6]naphthyridin-1-ylamino]ethanol (13n). The title compound was prepared from **12g** and cyclohexylamine by analogy to the method described for the preparation of **13e** above: MS (ESI) m/z 363.4 (M + 1); ^{1}H NMR (400 MHz, CD_3OD) δ ppm 9.21 (s, 1 H), 8.56 (d, 1 H), 8.04 (m, 2 H), 7.66 (s, 1 H), 7.22 (m, 2 H), 3.93 (m, 4 H), 3.74 (m, 2 H), 2.08 (m, 2 H), 1.84 (m, 2 H), 1.73 (m, 1 H), 1.51 (m, 2 H), 1.32 (m, 4 H).

4-[3-(2-Cyclohexylaminopyridin-4-yl)[2,6]naphthyridin-1-yl]piperazin-2-one (13o). The title compound was prepared from **12h** and cyclohexylamine by analogy to the method described for the preparation of **13e** above: MS (ESI) m/z 403.3 (M + 1).

{1-[3-(2-Cyclohexylaminopyridin-4-yl)[2,6]naphthyridin-1-yl]-piperidin-4-ylmethyl}carbamic Acid *tert*-Butyl Ester (13p). The title compound was prepared from **12i** and cyclohexylamine by analogy to the method described for the preparation of **13e** above: MS (ESI) m/z 417.2 (M + 1).

1-[3-(2-Cyclohexylaminopyridin-4-yl)[2,6]naphthyridin-1-yl]-piperidine-4-carboxylic Acid Piperidin-4-ylamide (13q). The title compound was prepared from **13p** by reaction with TFA/CH_2Cl_2 according to the method outlined for the preparation of **13c** above: MS (ESI) m/z 514.3 (M + 1); ^{1}H NMR (400 MHz, DMSO-d_6) δ ppm 9.36 (s, 1 H), 8.61 (d, J = 5.8 Hz, 1 H), 8.05 (d, J = 5.6 Hz, 1 H), 8.03 (s, 1 H), 7.86 (d, J = 5.8 Hz, 1 H), 7.80 (d, J = 7.8 Hz, 1 H), 7.28 (s, 1 H), 7.14 (dd, J = 5.4, 1.5 Hz, 1 H), 6.50 (d, J = 7.8 Hz, 1 H), 4.03 (m, 2 H), 374 (m, 1 H), 3.63 (m, 1 H), 3.00 (m, 4 H), 2.58 (m, 2 H), 2.40 (m, 1 H), 1.89 (m, 6 H), 1.72 (m, 4 H), 1.59 (m, 1 H), 1.26 (m, 8 H).

2-Amino-1-(4-{3-[2-(tetrahydropyran-4-ylamino)pyridin-4-yl]-[2,6]naphthyridin-1-yl}piperazin-1-yl)ethanone (13r). Compound **13f** (250 mg, 0.64 mmol) and HBTU (366 mg, 0.97 mmol) were dissolved in DMF (3 mL). Triethylamine (89 μL, 0.64 mmol) was added, and the mixture was stirred for 12 h. The mixture was concentrated under reduced pressure, and the residue was purified by flash chromatography to afford [2-oxo-2-(4-{3-[2-(tetrahydropyran-4-ylamino)pyridin-4-yl][2,6]naphthyridin-1-yl}piperazin-1-yl)ethyl]carbamic acid *tert*-butyl ester.

The BOC-protected amine above (267 mg, 0.49 mmol) was stirred in formic acid (5 mL) at room temperature. After 20 h, the mixture was concentrated under reduced pressure. The residue was purified by HPLC to afford the title compound: HRMS (ESI) m/z 448.2459 (M + 1); ^{1}H NMR (400 MHz,

$CDCl_3$) δ ppm 9.31 (s, 1 H), 8.66 (d, J = 5.8 Hz, 1 H), 8.21 (d, J = 5.4 Hz, 1 H), 7.83 (s, 1 H), 7.80 (d, J = 5.8 Hz, 1 H), 7.23 (dd, J = 5.4, 0.9 Hz, 1 H), 7.16 (s, 1 H), 4.55 (d, J = 7.9 Hz, 1 H), 4.11−3.98 (m, 3 H), 3.98−3.91 (m, 2 H), 3.74−3.66 (m, 2 H), 3.64−3.53 (m, 8 H), 2.11 (dd, J = 12.5, 1.9 Hz, 2 H), 1.70 (br s, 2 H), 1.63−1.51 (m, 2 H).

1-[3-(2-Cyclohexylaminopyridin-4-yl)[2,6]naphthyridin-1-yl]-piperidine-4-carboxylic Acid Amide (13s). The title compound was prepared from **12j** and cyclohexylamine by analogy to the method described for the preparation of **13e** above: MS (ESI) m/z 431.2 (M + 1); ^{1}H NMR (400 MHz, CD_3OD) δ ppm 9.22 (d, 1 H), 8.56 (d, 1 H), 7.98 (d, 1 H), 7.90 (br m, 2 H), 7.31 (d, 1 H), 7.18 (d, 1 H), 4.01 (br d, 2 H), 3.61 (m, 1 H), 3.08 (dd, 2 H), 2.58 (m, 1 H), 2.01−1.92 (br m, 6 H), 1.71 (br d, 2 H), 1.60 (d, 1 H), 1.37 (m, 2 H), 1.19 (m, 3 H).

1-{3-[2-(Tetrahydropyran-4-ylamino)pyridin-4-yl][2,6]naphthyridin-1-yl}piperidine-4-carboxylic Acid Amide (13t). The title compound was prepared from **12j** and 4-aminotetrahydropyran by analogy to the method described for the preparation of **13e** above: MS (ESI) m/z 433.3 (M + 1); ^{1}H NMR (400 MHz, DMSO-d_6) δ ppm 9.36 (s, 1 H), 8.63 (d, J = 6.1 Hz, 1 H), 8.07 (m, 2 H), 7.86 (d, J = 5.6 Hz, 1 H), 7.34 (s, 2 H), 7.19 (d, J = 4.0 Hz, 1 H), 6.83 (s, 1 H), 6.70 (br s, 1 H), 4.00 (m, 3 H), 3.89 (br dt, J = 8.0, 3.2 Hz, 2 H), 3.43 (td, J = 11.0, 2.0 Hz, 2 H), 3.40 (m, 1 H), 3.06 (m, 2 H), 2.42 (m, 1 H), 1.91 (br m, 5 H), 1.47 (m, 2 H).

1-[3-(2-Cyclohexylaminopyridin-4-yl)[2,6]naphthyridin-1-yl]piperidine-4-carboxylic Acid Methylamide (13u). The title compound was prepared from **12k** and cyclohexylamine by analogy to the method described for the preparation of **13e** above: MS (ESI) m/z 445.4 (M + 1); ^{1}H NMR (400 MHz, CD_3OD) δ ppm 9.28 (s, 1 H), 8.57 (d, 1 H), 8.00 (m, 2 H), 7.99 (d, 1 H), 7.38 (s, 1 H), 7.26 (d, 1 H), 4.13 (br d, 2 H), 3.68 (m, 1 H), 3.14 (dd, 2 H), 2.77 (s, 3 H), 2.50 (m, 1 H), 2.07 (br m, 4 H), 1.95 (m, 2 H), 1.80, (m, 2 H), 1.69 (br d, 1 H), 1.46 (m, 2 H), 1.29 (m, 3 H).

1-[3-(2-Cyclohexylaminopyridin-4-yl)[2,6]naphthyridin-1-yl]piperidine-4-carboxylic Acid (2-Pyrrolidin-1-ylethyl)amide (13v). The title compound was prepared from ester **12l** by the method outlined for the preparation of **13y** below: MS (ESI) m/z 528.4 (M + 1); ^{1}H NMR (400 MHz, DMSO-d_6) δ ppm 9.36 (s, 1 H), 8.62 (d, J = 5.3 Hz, 1 H), 8.03 (m, 2 H), 7.83 (m, 2 H), 7.29 (s, 1 H), 7.14 (d, J = 5.8 Hz, 1 H), 6.51 (d, J = 7.6 Hz, 1 H), 4.01 (m, 2 H), 3.74 (br s, 1 H), 3.18 (m, 2 H), 3.03 (m, 2 H), 1.92 (m, 8 H), 1.79−1.56 (m, 8 H), 1.42−1.10 (m, 8 H).

{1-[3-(2-Cyclohexylaminopyridin-4-yl)[2,6]naphthyridin-1-yl]piperidin-4-yl}-(4-hydroxypiperidin-1-yl)methanone (13w). A mixture of ester **12k** (500 mg, 1.3 mmol), 4-hydroxycyclohexylamine (400 mg, 3.9 mmol), and Me_3Al (4 mL of a 2 M solution, 8 mmol) in toluene (10 mL) was heated for 6 h at 110 °C. After cooling, the mixture was poured into MeOH (250 mL) and stirred for 10 min. The mixture was filtered and concentrated under reduced pressure. The residue was purified by flash chromatography (1−2% MeOH/CH_2Cl_2) to afford the amide as a yellow solid.

The amide above was converted to the target by coupling to cyclohexylamine using the method outlined for the preparation of **13e** above: MS (ESI) m/z 515.4 (M + 1); ^{1}H NMR (400 MHz, CD_3OD) δ ppm 9.27 (s, 1 H), 8.56 (d, J = 5.8 Hz, 1 H), 8.02−7.90 (m, 3 H), 7.37 (s, 1 H), 7.25 (d, J = 5.6 Hz, 1 H), 4.18−4.07 (m, 2 H), 4.02−3.93 (m, 1 H), 3.92−3.83 (m, 1 H), 3.75−3.63 (m, 1 H), 3.45−3.34 (m, 1 H), 3.27−3.10 (m, 3 H), 3.09−2.98 (m, 1 H), 2.17−1.96 (m, 4 H), 2.00−1.76 (m, 6 H), 1.75−1.62 (m, 1 H), 1.59−1.38 (m, 4 H), 1.36−1.21 (m, 4 H).

1-{3-[2-(Tetrahydropyran-4-ylamino)pyridin-4-yl][2,6]naphthyridin-1-yl}piperidine-4-carboxylic Acid Ethylamide (13x). The title compound was prepared from ester **12l** by the method outlined for the preparation of **13y** below: MS (ESI) 461.2 m/z (M + 1); ^{1}H NMR (400 MHz, MeOD) (TFA salt) δ ppm 8.68 (d, J = 5.8 Hz, 1 H), 8.22 (s, 1 H), 8.02 (d, J = 6.1 Hz, 1 H), 8.00−7.96 (m, 1 H), 7.95−7.86 (m, 1 H), 7.69−7.61 (m, 1 H), 4.26−4.16 (m, 2 H), 4.09−3.99 (m, 2 H), 3.96−3.84 (m, 1 H), 3.63−3.53 (m, 2 H), 3.29−3.14 (m, 4 H), 2.58−2.45 (m, 1 H), 2.15−2.01 (m, 4 H), 1.98−1.88 (m, 2 H), 1.79−1.64 (m, 2 H), 1.14 (t, J = 7.3 Hz, 3 H).

1-{3-[2-(Tetrahydropyran-4-ylamino)pyridin-4-yl][2,6]naphthyridin-1-yl}piperidine-4-carboxylic Acid Isopropylamide (13y). To a solution of **12k** (2.65 g, 6.93 mmol), THF (30 mL), and H_2O (10 mL) was added $LiOH \cdot H_2O$ (1.45 g, 34.6 mmol). After 20 min, an additional 30 mL of THF was added. After 5 h, the mixture was complete as judged by LCMS. At that point, 1 M HCl in Et_2O (35 mL) was added. The mixture was stirred for 10 min and then concentrated in vacuo. The residue was then azeotroped with toluene (3 × 150 mL) to give 1-[3-(2-chloropyridin-4-yl)[2,6]naphthyridin-1-yl]piperidine-4-carboxylic acid. The crude 1-[3-(2-chloropyridin-4-yl)[2,6]naphthyridin-1-yl]piperidine-4-carboxylic acid was taken up in DMF (60 mL) before DIEA (5.75 mL, 34.60 mmol), i-$PrNH_2$ (2.9 mL, 34.6 mmol), PyBOP (10.80 g, 20.80 mmol), and HOBt (0.94 g, 6.93 mmol) were added in sequence. The mixture was stirred at room temperature for 24 h, then concentrated in vacuo. The residue was taken up in CH_2Cl_2 (500 mL) and H_2O (500 mL). The layers were mixed and then separated. The aqueous layer was extracted further with CH_2Cl_2 (2 × 500 mL), and each organic layer was washed with an aliquot of H_2O (500 mL). The combined organic layers were then dried over Na_2SO_4, filtered, and concentrated. The residue was stirred with hot EtOAc (50 mL) and then filtered. The filtrate was then washed several times with cold EtOAc to give 1-[3-(2-chloropyridin-4-yl)[2,6]naphthyridin-1-yl]piperidine-4-carboxylic acid isopropylamide as a white solid: MS (ESI) m/z 410.2 (M + 1); ^{1}H NMR (400 MHz, DMSO-d_6) δ ppm 9.36 (s, 1 H), 8.68 (d, J = 5.8 Hz, 1 H), 8.56 (d, J = 5.3 Hz, 1 H), 8.38 (s, 1 H), 8.23 (s, 1 H), 8.20−8.15 (m, 1 H), 7.90 (d, J = 5.8 Hz, 1 H), 7.71 (d, J = 7.6 Hz, 1 H), 4.06 (d, J = 13.1 Hz, 2 H), 3.94−3.79 (m, 1 H), 3.13−3.02 (m, 2 H), 2.47−2.34 (m, 1 H), 2.00−1.81 (m, 4 H), 1.07 (d, J = 6.6 Hz, 6 H).

A pressure reaction vessel was charged with 1-[3-(2-chloropyridin-4-yl)[2,6]naphthyridin-1-yl]piperidine-4-carboxylic acid isopropylamide (0.50 g, 1.22 mmol), 4-aminotetrahydropyran (0.25 g, 2.44 mmol), Pd(t-Bu_3P)$_2$ (0.06 g, 0.12 mmol), t-BuONa (0.35 g, 3.66 mmol), and 1,4-dioxane. The mixture was sparged with argon for 10 min, and the vessel is then sealed and heated to 130 °C for 2.5 h. The contents of the vessel are allowed to cool to room temperature before being diluted with CH_2Cl_2 (150 mL) and brine (150 mL). The layers were mixed and then separated. The aqueous layer was extracted further with CH_2Cl_2 (3 × 150 mL), and the combined organic layers were then dried over Na_2SO_4, filtered, and concentrated. The residue was then separated via RP-HPLC (5−60% CH_3CN/H_2O/0.1% NH_4OH gradient) to give the title compound: MS (ESI) 475.1 m/z (M + 1); ^{1}H NMR (400 MHz, DMSO-d_6) δ ppm 9.36 (s, 1 H), 8.62 (d, J = 5.6 Hz, 1 H), 8.08 (d, J = 5.3 Hz, 1 H), 8.04 (s, 1 H), 7.86 (d, J = 5.8 Hz, 1 H), 7.70 (d, J = 7.6 Hz, 1 H), 7.31 (s, 1 H), 7.22−7.14 (m, 1 H), 6.66 (d, J = 7.6 Hz, 1 H), 4.09−3.93 (m, 3 H), 3.94−3.77 (m, 3 H), 3.49−3.36 (m, 2 H), 3.05 (t, J = 12.0 Hz, 2 H), 2.46−2.31 (m, 1) H, 2.01−1.78 (m, 6 H), 1.56−1.38 (m, 2 H), 1.07 (d, J = 6.6 Hz, 6 H).

1-{3-[2-(Tetrahydropyran-4-ylamino)pyridin-4-yl][2,6]naphthyridin-1-yl}piperidine-4-carboxylic Acid Isobutylamide (13z). The title compound was prepared from ester **12k** by the method outlined for the preparation of **13y** above: MS (ESI) m/z 489.2 (M + 1); ^{1}H NMR (400 MHz, $CDCl_3$) δ ppm 9.27 (s, 1 H), 8.62 (d, J = 5.8 Hz, 1 H), 8.20 (d, J = 5.6 Hz, 1 H), 7.79 (d, J = 5.8 Hz, 1 H), 7.76 (s, 1 H), 7.26−7.22 (m, 1 H), 7.20 (s, 1 H), 5.58 (t, J = 5.6 Hz, 1 H), 4.50 (d, J = 8.1 Hz, 1 H), 4.14−3.98 (m, 5 H), 3.65−3.54 (m, 2 H), 3.19−3.07 (m, 4 H), 2.46−2.33 (m, 1 H), 2.22−2.01 (m, 6 H), 1.87−1.75 (m, 1 H), 0.95 (d, J = 6.6 Hz, 6 H).

1-{3-[2-(Tetrahydropyran-4-ylamino)pyridin-4-yl][2,6]naphthyridin-1-yl}piperidine-4-carboxylic Acid (2-Pyrrolidin-1-ylethyl)-amide (13aa). The title compound was prepared from ester **12k** by the method outlined for the preparation of **13y** above: MS (ESI) m/z 530.4 (M + 1); ^{1}H NMR (400 MHz, DMSO-d_6) δ ppm 9.29 (s, 1 H), 8.55 (d, J = 5.8 Hz, 1 H), 8.00 (d, J = 5.6 Hz, 1 H), 7.98

(s, 1 H), 7.84−7.71 (m, 2 H), 7.25 (s, 1 H), 7.11 (d, J = 5.6 Hz, 1 H), 6.59 (d, J = 7.6 Hz, 1 H), 3.87−4.01 (m, 3 H), 3.87−3.78 (m, 2 H), 3.41−3.30 (m, 2 H), 3.12 (d, J = 19.2 Hz, 2 H), 2.99 (d, J = 23.2 Hz, 2 H), 1.92−1.74 (m, 8 H), 1.60 (br s, 4 H), 1.49−1.28 (m, 6 H).

1-{3-[2-(Tetrahydropyran-4-ylamino)pyridin-4-yl][2,6]naphthyridin-1-yl}piperidine-4-carboxylic Acid (2-*tert*-Butoxyethyl)-amide (13ab). The title compound was prepared from ester **12k** by the method outlined for the preparation of **13y** above: MS (ESI) m/z 533.2 (M + 1); ^{1}H NMR (400 MHz, $CDCl_3$) δ ppm 9.27 (s, 1 H), 8.63 (d, J = 5.8 Hz, 1 H), 8.20 (d, J = 5.3 Hz, 1 H), 7.79 (d, J = 5.8 Hz, 1 H), 7.76 (s, 1 H), 7.25−7.22 (m, 1 H), 7.20 (s, 1 H), 6.01 (br s, 1 H), 4.54−4.46 (m, 1 H), 4.15−3.97 (m, 5 H), 3.65−3.54 (m, 2 H), 3.49−3.44 (m, 4 H), 3.19−3.07 (m, 2 H), 2.49−2.34 (m, 1 H), 2.18−1.97 (m, 6 H), 1.21 (s, 9 H).

1-{3-[2-(Tetrahydropyran-4-ylamino)pyridin-4-yl][2,6]naphthyridin-1-yl}piperidine-4-carboxylic Acid (2-Hydroxyethyl)amide (13ac). The title compound was prepared from **13ab** above by acidic deprotection (TFA in CH_2Cl_2) of the *tert*-butyl ether to afford the title alcohol: MS (ESI) m/z 477.1 (M + 1); ^{1}H NMR (400 MHz, $CDCl_3$) δ ppm 9.29 (s, 1 H), 8.65 (d, J = 5.6 Hz, 1 H), 8.22−8.15 (m, 1 H), 7.83−7.76 (m, 2 H), 7.27−7.24 (m, 2 H), 6.08−5.99 (m, 1 H), 4.17−3.98 (m, 5 H), 3.84−3.76 (m, 2 H), 3.67−3.57 (m, 2 H), 3.56−3.47 (m, 2 H), 3.20−3.09 (m, 2 H), 2.53−2.41 (m, 1 H), 2.39−2.26 (m, 1 H), 2.23−2.02 (m, 7 H), 1.70−1.60 (m, 2 H).

4-({1-[3-(2-Cyclohexylaminopyridin-4-yl)[2,6]naphthyridin-1-yl]-piperidine-4-carbonyl}amino)piperidine-1-carboxylic Acid *tert*-Butyl Ester (13ad). The title compound was prepared from ester **12k** by the method outlined for the preparation of **13y** above: MS (ESI) m/z 614.4 (M + 1).

1-[3-(2-Cyclohexylaminopyridin-4-yl)[2,6]naphthyridin-1-yl]-piperidine-4-carboxylic Acid Piperidin-4-ylamide (13ae). The title compound was prepared from **13ad** above by acidic deprotection (TFA in CH_2Cl_2) to afford the title amine: MS (ESI) m/z 514.3 (M + 1); ^{1}H NMR (400 MHz, DMSO-d_6) δ ppm 9.36 (s, 1 H), 8.61 (d, J = 5.8 Hz, 1 H), 8.05 (d, J = 5.6 Hz, 1 H), 8.03 (s, 1 H), 7.86 (d, J = 5.8 Hz, 1 H), 7.80 (d, J = 7.8 Hz, 1 H), 7.28 (s, 1 H), 7.14 (dd, J = 5.4, 1.5 Hz, 1 H), 6.50 (d, J = 7.8 Hz, 1 H), 4.09−3.96 (m, 2 H), 3.82−3.66 (m, 1 H), 3.69−3.57 (m, 1 H), 3.11−2.92 (m, 4 H), 2.64−2.52 (m, 2 H), 2.46−2.34 (m, 1 H), 2.00−1.79 (m, 6 H), 1.78−1.66 (m, 4 H), 1.66−1.53 (m, 1 H), 1.40−1.12 (m, 8 H).

***N*-*tert*-Butyl-2-methylbenzamide (14a).** To an ice-cold solution of aqueous Na_2CO_3 (1 M, 30 mL) containing *tert*-butylamine (3.2 mL, 30 mmol) was added 2-methylbenzoyl chloride (3.9 g, 25 mmol) in dioxane (5 mL) slowly dropwise. After the addition, the mixture was allowed to warm to room temperature and further stirred for 4 h. The resulting slurry was diluted with water and the precipitate was filtered and air-dried to give **14a** as a white solid (3.6 g, 75%) matching the reported ^{1}H NMR data.[26]

3-Methylpyridine-2-carboxylic Acid *tert*-Butylamide (14b). To a solution of 2-cyano-3-methylpyridine (1.2 g, 12 mmol) in *tert*-butyl acetate (10 mL) was added concentrated H_2SO_4 (1 mL), and the mixture was stirred at room temperature overnight before it was diluted with water. The mixture was then carefully neutralized by adding NH_4OH at 0 °C and then extracted twice with 1:1 hexane−EtOAc. The combined organics were washed with saturated brine, dried (Na_2SO_4), filtered, and concentrated. The residue was chromatographed on silica gel to give **14b** as a colorless oil (1.85 g, 95%): ^{1}H NMR (400 MHz, $CDCl_3$) δ ppm 8.35 (d, J = 4.3 Hz, 1 H), 8.2 (br s, 1 H), 7.55 (m, 1 H), 7.27 (m, 1 H), 2.74 (s, 3 H), 1.48 (s, 9 H).

***N*-*tert*-Butyl-4-methylnicotinamide (14c).** The title compound was prepared in an analogous manner to the method described for the preparation of **14b** above: ^{1}H NMR (400 MHz, $CDCl_3$) δ ppm 8.52 (s, 1 H), 8.46 (d, J = 5.1 Hz, 1 H), 7.13 (d, J = 5.1 Hz, 1 H), 5.63 (br s, 1 H), 2.45 (s, 3 H), 1.48 (s, 9 H).

3-(2-Chloropyridin-4-yl)isochromen-1-one (15a). To a solution of **14a** (3.4 g, 18 mmol) in THF (60 mL) at −78 °C was added *n*-butyllithium (2.5 M in hexane, 16 mL, 40 mmol) slowly dropwise. After 30 min at −78 °C, ethyl 2-chloroisonicotinate (3.0 g, 17.4 mmol) in THF (10 mL) was added rapidly dropwise. The mixture was further stirred at −78 °C for 30 min before being quenched with AcOH (10 mL). The mixture was allowed to warm to room temperature and then concentrated in vacuo to remove volatiles. The residue was dissolved in AcOH (50 mL), and the mixture was heated at 80 °C with stirring. After cooling to room temperature, the resulting slurry was diluted with MeOH (50 mL) and the precipitate was collected by filtration, washed with MeOH, and air-dried to give **15a** as a white powder (2.8 g, 63%): MS (ESI) m/z 258.1 (M + 1); ^{1}H NMR (400 MHz, DMSO-d_6) δ ppm 8.72 (d, J = 5.3 Hz, 1 H), 8.38 (d, J = 7.9 Hz, 1 H), 8.2−8.0 (m, 4 H), 8.0−7.8 (m, 2 H).

3-[2-(2-Chloropyridin-4-yl)-2-oxoethyl]pyridine-2-carboxylic Acid *tert*-Butylamide (15b). The title compound was prepared from **14b** in a manner analogous to the method described above for the preparation of **15a**: ^{1}H NMR (400 MHz, DMSO-d_6) δ ppm 8.83 (s, 1 H), 8.58 (d, J = 5.2 Hz, 1 H), 8.35 (d, J = 8.3 Hz, 1 H), 8.22 (s, 1 H), 8.20−8.15 (m, 2 H), 8.00−7.90 (m, 2 H).

***N*-*tert*-Butyl-4-[2-(2-chloropyridin-4-yl)-2-oxoethyl]nicotinamide (15c).** The title compound was prepared from **14c** in a manner analogous to the method described above for the preparation of **15a**: MS (ESI) m/z 259.1 (M + 1); ^{1}H NMR (400 MHz, DMSO-d_6) δ ppm 9.68 (s, 1 H), 9.3 (d, J = 4.8 Hz, 1 H), 8.96 (d, J = 5.3 Hz, 1 H), 8.34 (s, 1 H), 8.24 (m, 2 H), 8.00 (d, J = 5.3 Hz, 1 H).

***N*-*tert*-Butyl-2-[2-(2-chloropyridin-4-yl)-2-oxoethyl]nicotinamide (15d).** The title compound was prepared from **14d** in a manner analogous to the method described above for the preparation of **15a**: ^{1}H NMR (400 MHz, DMSO-d_6) δ ppm 9.38 (dd, J = 4.4, 1.5 Hz, 1 H), 8.90 (d, 5.2 Hz, 1 H), 8.86 (d, J = 8.0 Hz, 1 H), 8.38 (s, 1 H), 8.29 (dd, J = 5.2, 1.5 Hz, 1 H), 8.21 (s, 1 H), 8.0 (dd, J = 8.0, 4.4 Hz, 1 H).

3-(2-Chloropyridin-4-yl)isoquinolin-1-ol (16a). To a suspension of **15a** (2.8 g, 11 mmol) in MeOH (10 mL) was added a 2 M solution of NH_3 in MeOH (40 mL). The mixture was heated to 80 °C in a sealed tube, and after it was cooled, the precipitate was collected by filtration. The crude product, which LCMS analysis indicated to be a 1:1 mixture of **16a** and uncyclized amide, was resuspended in MeOH. Concentrated HCl (0.1 mL) was added, and the mixture was heated to 60 °C for 1 h. The resulting slurry was cooled to 0 °C, filtered, washed with cold MeOH, and air-dried to give **16a** as a yellowish solid (2.6 g, 93%): MS (ESI) m/z 257.1 (M + 1); ^{1}H NMR (400 MHz, DMSO-d_6) δ ppm 11.65 (br, 1 H), 8.52 (d, J = 5.3 Hz, 1 H), 8.24 (d, J = 8.0 Hz, 1 H), 8.00 (s, 1 H), 7.87 (d, J = 5.5 Hz, 1 H), 7.77 (m, 2 H), 7.58 (m, 1 H), 7.3 (s, 1 H).

6-(2-Chloropyridin-4-yl)[1,7]naphthyridin-8-ol (16b). The title compound was prepared from **15b** by analogy to the method described above for the preparation of **16a**: MS (ESI) m/z 258.1 (M + 1); ^{1}H NMR (400 MHz, DMSO-d_6) δ ppm 12.22 (br s, 1 H), 9.15 (d, J = 4.0 Hz, 1 H), 8.87 (d, J = 5.6 Hz, 1 H), 8.51 (d, J = 8.1 Hz, 1 H), 8.32 (s, 1 H), 8.18 (d, J = 5.1 Hz, 1 H), 8.07 (dd, J = 8.1, 4.0 Hz, 1 H), 7.58 (s, 1 H).

3-(2-Chloropyridin-4-yl)[2,7]naphthyridin-1-ol (16c). The title compound was prepared from **15c** by analogy to the method described above for the preparation of **16a**: MS (ESI) m/z 258.1 (M + 1); ^{1}H NMR (400 MHz, DMSO-d_6) δ ppm 12.38 (br s, 1 H), 9.75 (s, 1 H), 9.17 (d, J = 4.6 Hz, 1 H), 8.95 (d, J = 5.6 Hz, 1 H), 8.38 (s, 1 H), 8.24 (d, J = 5.1 Hz, 1 H), 8.04 (d, J = 5.6 Hz, 1 H), 7.61 (s, 1 H).

7-(2-Chloropyridin-4-yl)[1,6]naphthyridin-5-ol (16d). The title compound was prepared from **15d** by analogy to the method described above for the preparation of **16a**: MS (ESI) m/z 258.1 (M + 1); ^{1}H NMR (400 MHz, DMSO-d_6) δ ppm 12.27 (br s, 1 H), 9.18 (d, 1 H), 8.89 (d, J = 5.1 Hz, 1 H), 8.53 (d, J = 8.1 Hz, 1 H), 8.34 (s, 1 H), 8.20 (d, J = 5.6 Hz, 1 H), 8.09 (dd, J = 8.1, 4.6 Hz, 1 H), 7.60 (s, 1 H).

2-(2-Chloropyridin-4-yl)quinazolin-4-ol (20). To a solution of **17** (6 g, 43 mmol) in dioxane (50 mL) was added MeOH (7 mL,

172 mmol), followed by 4 M HCl in dioxane (50 mL, 200 mmol). The mixture was stirred at room temperature overnight, and the resulting slurry was filtered, washed with dioxane, and air-dried to give crude imidate salt **18**. To an ice-cold solution of the crude **18** obtained as above in MeOH (50 mL) was added Na metal (2 g, 86 mmol) slowly in small pieces. After the addition, the mixture was heated to reflux with **19** for 6 h before it was allowed to cool to room temperature and filtered, washed with water, and air-dried to give the quinazolone **20**, which was used in the next step without further purification (4.6 g, 42%).

1-(1-Piperazinyl)-3-(2-cyclohexylaminopyrid-4-yl)isoquinoline (22a). A suspension of the above **16a** (510 mg, 1.99 mmol) in $POCl_3$ was heated at 100 °C with stirring for 2 h. After cooling to room temperature, the mixture was concentrated under reduced pressure, triturated with water, filtered, and air-dried to a yellow solid. The solid was dissolved in CH_2Cl_2, washed with a saturated aqueous solution of $NaHCO_3$, dried (Na_2SO_4), and filtered through silica gel to afford 1-chloro-3-(2-chloropyridin-4-yl)isoquinoline (0.47 g, 86%): MS (ESI) m/z 259.1 (M + 1); ^{1}H NMR (400 MHz, $CDCl_3$) δ ppm 8.83 (s, 1 H), 8.58 (d, J = 5.2 Hz, 1 H), 8.35 (d, J = 8.3 Hz, 1 H), 8.22 (s, 1 H), 8.20−8.15 (m, 2 H), 7.99 (dd, J = 8.3, 7.0 Hz, 1 H), 7.91 (dd, J = 8.3, 7.1 Hz, 1 H).

The 1-chloroisoquinoline above (360 mg, 1.3 mmol) and *N*-BOC piperazine (300 mg, 1.6 mmol) in NMP (1 mL) were heated to 180 °C in a microwave reactor for 45 min. After cooling, the mixture was poured into water and the resulting precipitate was isolated by filtration. The collected tan solid was dissolved in CH_2Cl_2 and purified by column chromatography using a gradient of 0−20% EtOAc/CH_2Cl_2. Compound **21a** was isolated as a solid 285 mg (51%): MS (ESI) m/z 425.3 (M + 1); ^{1}H NMR (400 MHz, $CDCl_3$) δ ppm 8.47 (d, J = 5.2 Hz, 1 H), 8.11 (d, J = 8.1 Hz, 1 H), 8.08 (s, 1 H), 7.94 (dd, J = 5.2, 1.5 Hz, 1 H), 7.87 (d, J = 8.1 Hz, 1 H), 7.82 (s, 1 H), 7.68 (dd, J = 7.5, 6.9 Hz, 1 H), 7.59 (dd, J = 8.1, 7.6 Hz, 1 H), 3.74 (m, 4 H), 3.50 (m, 4 H), 1.52 (s, 9 H).

A vial containing **21a** (42 mg, 0.1 mmol) in toluene (0.5 mL) and cyclohexylamine (12 mg, 0.12 mmol) in toluene (0.6 mL) was degassed with N_2. To the vial was added $Pd(OAc)_2$ and BINAP (0.25 mL of a 0.01 M solution in toluene, 2.5×10^{-3} mmol) followed by *t*-BuOK (0.12 mL of a 1 M solution in THF, 0.12 mmol). The vial was heated at 80 °C overnight. After cooling, the mixture was partitioned between toluene and water. The toluene layer was dried (Na_2SO_4) and concentrated under reduced pressure. The residue was purified by flash chromatography and then by preparative TLC to afford cyclohexylaminopyridine.

The pure fractions of the above compound were dissolved in CH_2Cl_2 (2 mL) and TFA (0.4 mL). After being stirred at room temperature overnight, the mixture was concentrated in vacuo and partitioned between CH_2Cl_2 and a saturated aqueous solution of $NaHCO_3$. The phases were separated using a Biotage phase separator cartridge. The organic layer was concentrated in vacuo. The residue was purified using silica gel solid phase extraction to afford the title compound **22a**: MS (ESI) m/z 388.3 (M + H); ^{1}H NMR (400 MHz, DMSO-d_6) δ ppm 8.52 (d, J = 8.1 Hz, 1 H), 8.44 (d, J = 5.1 Hz, 1 H), 8.42−8.35 (m, 2 H), 8.13 (t, J = 8.1 Hz, 1 H), 8.03 (t, J = 8.1 Hz, 1 H), 7.68 (s, 1 H), 7.55 (d, J = 5.6 Hz, 1 H), 6.85 (d, J = 7.6 Hz, 1 H), 4.22−4.08 (m, 1 H), 3.96−3.86 (m, 4 H), 3.67−3.59 (m, 4 H), 3.29−3.16 (m, 1 H), 2.40−2.31 (m, 2 H), 2.19−2.07 (m, 2 H), 2.06−1.95 (m, 1 H), 1.82−1.67 (m, 2 H), 1.68−1.53 (m, 3 H).

Cyclohexyl-[4-(8-piperazin-1-yl[1,7]naphthyridin-6-yl)pyridin-2-yl]amine (22b). The title compound was prepared from **16b** by analogy to the method described for the preparation of **22a**. The intermediate **21b** was generated under milder conditions than **21a** above (80 °C, overnight): MS (ESI) m/z 259.1 (M + 1); ^{1}H NMR (400 MHz, $CDCl_3$) δ ppm 8.87 (dd, J = 4.2, 1.8 Hz, 1 H), 8.48 (d, J = 5.2 Hz, 1 H), 8.11 (dd, J = 8.3, 1.9 Hz, 1 H), 8.04 (d, J = 1.6 Hz, 1 H), 7.91 (dd, J = 5.2, 1.6 Hz, 1 H), 7.6 (s, 1 H), 7.56 (dd, J = 8.3, 4.2 Hz, 1 H), 4.12 (br, 4 H), 3.72 (m, 4 H), 1.51 (s, 9 H).

The title compound was prepared from **21b** by Buchwald amination followed by acidic deprotection: MS (ESI) m/z 389.4 (M + 1); ^{1}H NMR (400 MHz, DMSO-d_6) δ ppm 8.99 (d, J = 4.0 Hz, 1 H), 8.45 (d, J = 8.1 Hz, 1 H), 8.18 (d, J = 5.1 Hz, 1 H), 7.88 (s, 1 H), 7.82 (dd, J = 8.6, 3.54 Hz, 1 H), 7.41 (s, 1 H), 7.25 (d, J = 5.1 Hz, 1 H), 6.61 (d, J = 7.6 Hz, 1 H), 4.22−4.10 (m, 4 H), 3.98−3.84 (m, 1 H), 3.16−3.04 (m, 4 H), 2.16−2.05 (m, 2 H), 1.95−1.83 (m, 2 H), 1.80−1.70 (m, 1 H), 1.56−1.25 (m, 5 H).

Cyclohexyl-[4-(1-piperazin-1-yl[2,7]naphthyridin-3-yl)pyridin-2-yl]amine (22c). The title compound was prepared from **16c** by analogy to the method described for the preparation of **22b**. The intermediate **21c** was isolated as a solid: MS (ESI) m/z 426.2 (M + 1); ^{1}H NMR (400 MHz, $CDCl_3$) δ ppm 9.48 (s, 1 H), 8.69 (d, J = 5.7 Hz, 1 H), 8.50 (d, J = 5.2 Hz, 1 H), 8.05 (d, J = 1.5 Hz, 1 H), 7.91 (dd, J = 5.2, 1.5 Hz, 1 H), 7.69 (s, 1 H), 7.64 (d, J = 5.7 Hz, 1 H), 3.75 (m, 4 H), 3.65 (m, 4 H), 1.52 (s, 9 H).

Buchwald amination of **21c** followed by deprotection under acidic conditions afforded the title compound **22c**: MS (ESI) m/z 389.4 (M + 1); ^{1}H NMR (400 MHz, DMSO-d_6) δ ppm 9.67 (s, 1 H), 9.08 (br s, 2 H), 8.90−8.85 (m, 1 H), 8.24−8.17 (m, 2 H), 8.03 (d, J = 5.56 Hz, 1 H), 7.54 (br s, 1 H), 7.37 (br s, 1 H), 3.93 (br s, 4 H), 3.59 (br s, 4 H), 3.30−3.19 (m, 1 H), 2.13−2.07 (m, 2 H), 1.94−1.85 (m, 2 H), 1.82−1.72 (m, 1 H), 1.59−1.34 (m, 5 H).

Cyclohexyl-[4-(5-piperazin-1-yl[1,6]naphthyridin-7-yl)pyridin-2-yl]amine (22d). The title compound was prepared from **16d** by analogy to the method described for the preparation of **22a**: MS (ESI) m/z 389.3 (M + 1); ^{1}H NMR (400 MHz, DMSO-d_6) δ ppm 9.02 (dd, J = 4.2, 1.6 Hz, 1 H), 8.50−8.39 (m, 1 H), 8.05 (d, J = 5.3 Hz, 1 H), 7.90 (s, 1 H), 7.57 (dd, J = 8.5, 4.2 Hz, 1 H), 7.32 (d, J = 0.8 Hz, 1 H), 7.19 (dd, J = 5.4, 1.5 Hz, 1 H), 6.50 (d, J = 7.8 Hz, 1 H), 3.83−3.71 (m, 1 H), 3.47−3.39 (m, 4 H), 3.05−2.95 (m, 4 H), 2.02−1.90 (m, 2 H), 1.80−1.67 (m, 2 H), 1.66−1.57 (m, 1 H), 1.43−1.13 (m, 5 H).

Cyclohexyl-[4-(4-piperazin-1-ylquinazolin-2-yl)pyridin-2-yl]-amine (22e). The title compound was prepared from **20** by analogy to the method described for the preparation of **22a**. The intermediate **21e** was isolated as a solid: ^{1}H NMR (400 MHz, $CDCl_3$) δ ppm 8.52 (d, J = 5.2 Hz, 1 H), 8.41 (s, 1 H), 8.31 (dd, J = 5.1, 1.3 Hz, 1 H), 8.01 (d, J = 8.4 Hz, 1 H), 7.93 (d, J = 8.3 Hz, 1 H), 7.80 (app t, J = 8.3 Hz, 1 H), 7.52 (app t, J = 8.2 Hz, 1 H), 3.86 (m, 4 H), 3.71 (m, 4 H), 1.51 (s, 9 H).

Deprotection of **21e** was effected under acidic conditions to afford the title compound **22e** as a solid: MS (ESI) m/z 389.3 (M + 1); ^{1}H NMR (400 MHz, $CDCl_3$) δ ppm 8.19 (d, J = 5.1 Hz, 1 H), 7.98 (d, J = 8.1 Hz, 1 H), 7.91 (d, J = 8.6 Hz, 1 H), 7.74 (t, J = 7.3 Hz, 1 H), 7.61 (d, J = 6.1 Hz, 1 H), 7.52 (s, 1 H), 4.67 (br s, 1 H), 3.89−3.80 (m, 4 H), 3.80−3.68 (m, 1 H), 3.17−3.08 (m, 4 H), 2.17−2.07 (m, 2 H), 1.87−1.61 (m, 3 H), 1.33−1.19 (m, 3 H), 1.52−1.38 (m, 2 H).

Acknowledgment. We thank Patrick Cronan for high resolution mass spectrometry data, Analytical Sciences for LCMS and NMR support, and Angela Mackay for the preparation of **12g**. We thank the Metabolism and Pharmacokinetics Group for the in vivo and bioanalytical support in the pharmacokinetic studies.

Supporting Information Available: Figures S1 and S2 showing the PK iv and po curves for **13c** and **13y**; Table T1 listing percent activity remaining for kinases. This material is available free of charge via the Internet at http://pubs.acs.org.

References

(1) (a) Chatterjee, K.; Massie, B. Systolic and diastolic heart failure: differences and similarities. *J. Card. Failure* **2007**, *13*, 569. (b) Arai, M.; Koitabashi, N.; Watanabe, A.; Niwano, K.; Matsui, H.; Ohyama, Y.; Kurabayashi, M. Mechanisms that underlie diastolic heart failure and diastolic dysfunction. *J Card. Failure* **2008**, *14* (Suppl. 1), S142. (c) For WHO mortality data by country or region, see http://www.who.int/whosis/whostat2006_mortality.pdf.

(2) Hill, J. A.; Olson, E. N. Mechanisms of disease: cardiac plasticity. *N. Engl. J. Med.* **2008**, *358*, 1370–1380.
(3) Gosse, P. Left ventricular hypertrophy as a predictor of cardiovascular risk. *J. Hypertens.* **2005**, *23* (Suppl. 1), S27–S33.
(4) Devereux, R. B.; Wachtell, K.; Gerdts, E.; Boman, K.; Nieminen, M. S.; Papademetriou, V.; Rokkedal, J.; Harris, K.; Aurup, P.; Dahloef, B. Prognostic significance of left ventricular mass change during treatment of hypertension. *JAMA, J. Am. Med. Assoc.* **2004**, *292*, 2350–2356.
(5) Aurigemma, G. P; Zile, M. R.; Gaasch, W. H. Contractile behavior of the left ventricle in diastolic heart failure with emphasis on regional systolic function. *Circulation* **2006**, *113*, 296–304.
(6) (a) Frey, N.; Olson, E. N. Cardiac hypertrophy: the good, the bad, and the ugly. *Annu. Rev. Physiol.* **2003**, *65*, 45–79. (b) McKinsey, T. A.; Kass, D. A. Small-molecule therapies for cardiac hypertrophy: moving beneath the cell surface. *Nat. Rev. Drug Discovery* **2007**, *6*, 617–635.
(7) Potthoff, M. J.; Olson, E. N. MEF2: a central regulator of diverse developmental programs. *Development* **2007**, *134*, 4131–4140.
(8) Kim, Y.; Phan, D.; van Rooij, E.; Wang, D.-Z.; McAnally, J.; Qi, X.; Richardson, J. A.; Hill, J. A.; Bassel-Duby, R.; Olson, E. N. The MEF2D transcription factor mediates stress-dependent cardiac remodeling in mice. *J. Clin. Invest.* **2008**, *118*, 124–132.
(9) (a) Chang, S.; McKinsey, T. A.; Zhang, C. L.; Richardson, J. A.; Hill, J. A.; Olson, E. N. Histone deacetylases 5 and 9 govern responsiveness of the heart to a subset of stress signals and play redundant roles in heart development. *Mol. Cell. Biol.* **2004**, *24*, 8467–8476. (b) Olson, E. N.; Backs, J.; McKinsey, T. A. Control of cardiac hypertrophy and heart failure by histone acetylation/deacetylation. *Novartis Found. Symp.* **2006**, *274* (Heart Failure), 3–19.
(10) Harrison, B. C.; Roberts, C. R.; Hood, D. B.; Sweeney, M.; Gould, J. M.; Bush, E. W.; McKinsey, T. A. The CRM1 nuclear export receptor controls pathological cardiac gene expression. *Mol. Cell. Biol.* **2004**, *24*, 10636–10649.
(11) (a) Fielitz, J.; Kim, M.-S.; Shelton, J. M.; Qi, X.; Hill, J. A.; Richardson, J. A.; Bassel-Duby, R.; Olson, E. N. Requirement of protein kinase D1 for pathological cardiac remodeling. *Proc. Natl. Acad. Sci. U.S.A.* **2008**, *105*, 3059–3063. (b) Ha, C. H.; Wang, W.; Jhun, B. S.; Wong, C.; Hausser, A.; Pfizenmaier, K.; McKinsey, T. A.; Olson, E. N.; Jin, Z.-G. Protein kinase D-dependent phosphorylation and nuclear export of histone deacetylase 5 mediates vascular endothelial growth factor-induced gene expression and angiogenesis. *J. Biol. Chem.* **2008**, *283*, 14590–14599. (c) Backs, J.; Backs, T.; Bezprozvannaya, S.; McKinsey, T. A.; Olson, E. N. Histone deacetylase 5 acquires calcium/calmodulin-dependent kinase II responsiveness by oligomerization with histone deacetylase 4. *Mol. Cell. Biol.* **2008**, *28*, 3437–3445. (d) Huynh, Q. K.; McKinsey, T. A. Protein kinase D directly phosphorylates histone deacetylase 5 via a random sequential kinetic mechanism. *Arch. Biochem. Biophys.* **2006**, *450*, 141–148. (e) Vega, R. B.; Harrison, B. C.; Meadows, E.; Roberts, C. R.; Papst, P. J.; Olson, E. N.; McKinsey, T. A. Protein kinases C and D mediate agonist-dependent cardiac hypertrophy through nuclear export of histone deacetylase 5. *Mol. Cell. Biol.* **2004**, *24*, 8374–8385. (f) Monovich, L.; Vega, R. B.; Meredith, E.; Miranda, K.; Rao, C.; Capparelli, M.; Lemon, D. D.; Phan, D.; Koch, K. A.; Chapo, J. A.; Hood, D. B.; McKinsey, T. A. A novel kinase inhibitor establishes a predominant role for protein kinase D as a cardiac class IIa histone deacetylase kinase. *FEBS Lett.* **2010**, *584*, 631–637.
(12) Gschwendt, M.; Dieterich, S.; Rennecke, J.; Kittstein, W.; Mueller, H.-J.; Johannes, F.-J. Inhibition of protein kinase C μ by various inhibitors. Differentiation from protein kinase c isoenzymes. *FEBS Lett.* **1996**, *392*, 77.
(13) (a) Singh, R.; Li, H.; Zhao, H.; Payan, D. G.; Kolluri, R.; Tso, K.; Ramphal, J.; Gu, S. Preparation of Cyclic Amine Substituted Pyrimidinediamines as PKC Inhibitors. WO 2009012421, 2009. (b) Yokoyama, S. AP2 Inhibitor WO 2008088006, 2008. (c) Raynham, T. M.; Hammonds, T. R.; Charles, M. D.; Pave, G. A.; Foxton, C. H.; Blackaby, W. P.; Stevens, A. P.; Ekwuru, C. T. Pyridine Benzamides and Pyrazine Benzamides as PKD Inhibitors and Their Preparation, Pharmaceutical Compositions and Use in the Treatment of Diseases, WO 2008074997, 2008. (c) Raynham, T. M.; Hammonds, T. R.; Gilliatt, J. H.; Charles, M. D.; Pave, G. A.; Foxton, C. H.; Carr, J. L.; Mistry, N. S. Aminoethylamino-aryl (AEAA) Compounds as PKD Inhibitors and Their Preparation, Pharmaceutical Compositions and Use in the Treatment of PKD-Mediated Diseases. WO 2007125331, 2007. (d) Gschwendt, M.; Kittstein, W.; Johannes, F.-J. Differential effects of suramin on protein kinase C isoenzymes, a novel tool for discriminating protein kinase C activities. *FEBS Lett.* **1998**, *421*, 165–168.
(14) Sharlow, E. R.; Giridhar, K. V.; LaValle, C. R.; Chen, J.; Leimgruber, S.; Barrett, R.; Bravo-Altamirano, K.; Wipf, P.; Lazo, J. S.; Wang, Q. J. Potent and selective disruption of protein kinase D functionality by a benzoxoloazepinolone. *J. Biol. Chem.* **2008**, *283*, 33516–33526.
(15) Slater, S. J.; Seiz, J. L.; Cook, A. C.; Stagliano, B. A.; Buzas, C. J. Inhibition of protein kinase C by resveratrol. *Biochim. Biophys. Acta, Mol. Basis Dis.* **2003**, *1637*, 59–69.
(16) Haworth, R. S.; Avkiran, M. Inhibition of protein kinase D by resveratrol. *Biochem. Pharmacol.* **2001**, *62*, 1647–1651.
(17) Storz, P.; Doppler, H.; Toker, A. Activation loop phosphorylation controls protein kinase D-dependent activation of nuclear factor kappaB. *Mol. Pharmacol.* **2004**, *66*, 870–879.
(18) Rozengurt, E.; Rey, O.; Waldron, T. Protein kinase D signaling. *J. Biol. Chem.* **2005**, *280*, 13205–13208.
(19) Huang, D.; Zhou, T.; Lafleur, K.; Nevado, C.; Caflisch, A. Kinase selectivity potential for inhibitors targeting the ATP binding site: a network analysis. *Bioinformatics* **2010**, *26*, 198–204.
(20) Wang, Q. J. PKD at the crossroads of DAG and PKC signaling. *Trends Pharmacol. Sci.* **2006**, *27*, 317–323.
(21) Huynh, Q. K.; McKinsey, T. A. Protein kinase D directly phosphorylates histone deacetylase 5 via a random sequential kinetic mechansim. *Arch. Biochem. Biophys.* **2006**, *450*, 141–148.
(22) Izumi, Y.; Matsuoka, M.; Kubo, A.; Nakayama, T.; Fukuda, N.; Watanabe, Y.; Soma, M.; Kanmatsuse, K. Prevention of cardiac hypertrophy by a sub-antihypertensive dose of the α 1-adrenergic antagonist bunazosin in Dahl salt-sensitive rats. *Hypertens. Res.* **1996**, *19*, 147–150.
(23) Kobayashi, M.; Machida, N.; Mitsuishi, M.; Yamane, Y. β-Blocker improves survival, left ventricular function, and myocardial remodeling in hypertensive rats with diastolic heart failure. *Am. J. Hypertens.* **2004**, *17*, 1112–1119.
(24) Hardt, S. E.; Sadoshima, J. Negative regulators of cardiac hypertrophy. *Cardiovas. Res.* **2004**, 500–509.
(25) Meredith, E. L.; Beattie, K.; Burgis, R.; Capparelli, M.; Chapo, J.; DiPietro, L.; Gamber, G.; Enyedy, I.; Hood, D. B.; Hosagrahara, V.; Jewell, C.; Koch, K. A.; Lee, W.; Lemon, D. D.; McKinsey, T. A.; Miranda, K.; Pagratis, N.; Phan, D.; Plato, C.; Rao, C.; Rozhitskaya, O.; Soldermann, N.; Springer, C.; Van Eis, M.; Vega, R. B.; Yan, W.; Zhu, Q.; Monovich, L. Identification of potent and selective amidobipyridyl inhibitors of protein kinase D. *J. Med. Chem.* DOI: 10.1021/jm100076w.
(26) Houlihan, W. J.; Cheon, S. H.; Parrino, V. A.; Handley, D. A.; Larson, D. A. Structural modification of 5-aryl-2,3-dihydroimidazo[2,1-*a*]isoquinoline platelet activating factor receptor antagonists. *J. Med. Chem.* **1993**, *36*, 3098–3102.